International Journal of Bifurcation and Chaos, Vol. 20, No. 10 (2010) 3105–3135

DOI: 10.1142/S0218127410027581

CALCULATION OF BIFURCATION CURVES BY MAP REPLACEMENT

VIKTOR AVRUTIN and MICHAEL SCHANZ
Institute of Parallel and Distributed Systems, University of Stuttgart, Germany

LAURA GARDINI
Department of Economics, University of Urbino, Italy

Received December 17, 2009; Revised January 18, 2010

The complex bifurcation structure in the parameter space of the general piecewise-linear scalar map with a single discontinuity — nowadays known as nested period adding structure — was completely studied analytically by N. N. Leonov already 50 years ago. He used an elegant and very efficient recursive technique, which allows the analytical calculation of the border-collision bifurcation curves, causing the nested period adding structure to occur. In this work, we have demonstrated that the application of Leonov's technique is not resticted to that particular bifurcation structure. On the contrary, the presented map replacement approach, which is an extension of Leonov's technique, allows the analytical calculation of border-collision bifurcation curves for periodic orbits with high periods and complex symbolic sequences using appropriate composite maps and the bifurcation curves for periodic orbits with much lower periods.

Keywords: Discontinuous piecewise-linear 1D map; border collision bifurcation curves; map replacement technique; rested period adding; Farey structure.

1. Introduction and Historical Remarks

Nonsmooth models appear naturally in many application fields. Representative examples for systems where the adequate description of the dynamic behavior requires nonsmooth and often even discontinuous system functions, are electronic circuits with switching behavior, mechanical systems with suspensions, gears, transmissions, ball bearings where impacts or stick slip behavior occurs. Further examples range from economy where several business cycle models are nonsmooth, micro- and nano-technology in particular piezoelectric energy harvesting devices and devices using piezoelectric or other micro-machined actuators [Mita *et al.*, 2003; Zhao *et al.*, 2004] to generate movement or propulsion in a very precise manner up to several models [Karner, 1994; Saif *et al.*, 1998; Leonel & McClintock, 2006] of the Fermi accelerator [Fermi, 1949]. Additionally, the importance of nonsmooth systems is based on the fact that Poincaré return maps of continuous flows showing chaotic behavior are inherently discontinuous. It is also known that piecewise-smooth dynamical systems are able to demonstrate not only all phenomena which occur in smooth systems but also some additional phenomena which are therefore specific for these models. As the state space of piecewise-smooth systems is subdivided in several partitions, these phenomena are related with interactions between invariant sets of the system and the boundaries between these partitions in the state space. A typical example for that is given by border-collision bifurcations.

In the history of nonlinear dynamics border-collision bifurcations became a focus of research interest about 1990, after [Nusse & Yorke, 1992; Nusse *et al.*, 1994] where the term *border-collision bifurcation* was introduced. Nevertheless, there are

some earlier works on this topic published already in 1970 [Feigin, 1970] and in 1974 [Peterka, 1974a, 1974b] Nowadays their works will be frequently referred to as the first publications on border-collision related phenomena.

Surprisingly, this is not completely true. In fact, already in 1959 (that means, 50 years ago) the Russian mathematician N. N. Leonov published a series of works on nonsmooth maps and presented a number of fundamental results which remained mainly unknown until now.

In his works Leonov considered a four-parametric family of piecewise-linear discontinuous 1D maps defined on two partitions. It was demonstrated that the number of parameters which determine the dynamical behavior is in fact three and the bifurcation structure of the complete 3D parameter space was reported in detail. Not only the existence boundaries of specific periodic orbits were explained by introducing the bifurcations which are now referred to as border-collision bifurcations, but also the bifurcation scenarios formed by these orbits were reported. The parameter regions structured by these scenarios (denoted now as period adding and period increment) were identified. Regarding the period increment scenario, Leonov demonstrated that at most two stable periodic orbits corresponding to symbolic sequences $\mathcal{LR}^n$ or $\mathcal{RL}^n$ (which are now denoted as maximal, principal, basic or simple orbits) can coexist. Considering the period adding scenario, Leonov has not only determined the underlying structure in the space of symbolic sequences (known in the meanwhile as Farey- or Brocot-tree-like infinite symbolic sequences adding scheme, also denoted as the symbolic representation of the Farey tree), but has also shown that in the limiting case stable aperiodic dynamics is possible, although on a parameter subspace with zero Lebesgue measure.

Due to several reasons (including the language barrier) the results obtained by Leonov were not known by the scientific community (although they were reported in [Mira, 1987]) and were therefore mostly rediscovered later by other researchers. However, one idea used by Leonov for the analytical calculation of bifurcation curves within the period adding scenario is still not only of historical interest.

Since computer algebra software like Maple or Mathematica were not available at that time, Leonov used the following idea to simplify the calculation of border-collision bifurcation curves involving high-periodic orbits with complex symbolic sequences: first, he calculated the border-collision bifurcation of some other usually much simpler orbits. This was done in a way similar to what we call nowadays a straight forward calculation. Leonov noticed the fact that the existence region of each orbit is confined by two border-collision bifurcations. He calculated one of them using the condition that a fixed point of the iterated function collides with the boundary and the other one using the condition that the same fixed point collides with the image of the boundary. For details we refer to [Gardini *et al.*, 2010] where the steps performed by Leonov are explained and extended. Eventually he defined a different (composite) map related to the original one in an appropriate way (using some composite coefficients), so that the already calculated curves exist also in this new map and correspond in the original map to periodic orbits with usually more complex symbolic sequences. This can be seen as a two-steps approach: first the bifurcation curves calculated in the original parameter space will be transferred into a different parameter space by a simple replacement of coefficients, and after that, the obtained results will be mapped back to the original parameter space. This allowed Leonov to describe the period adding structure analytically with a surprisingly small calculation effort and in much more detail than it can be done by straight forward calculation.

In fact, the application of Leonov's ideas is neither restricted to period adding structures nor to border-collision bifurcations. In the presented work we ask the following question: which conditions must be fulfilled for the calculation of border-collision bifurcations of a periodic orbit with complex symbolic sequence based on border-collision bifurcations of a different periodic orbit with much simpler symbolic sequence. This will be done without any additional assumptions regarding the bifurcation scenarios both periodic orbits are involved in, and represents therefore a generalization of Leonov's approach, which we denote as the *map replacement approach*. For a further generalization regarding bifurcation types other than border-collision bifurcations, we refer to [Avrutin & Schanz, 2009] and to forthcoming works.

The presented work is structured as follows. In Sec. 2 we discuss the basic idea of the map replacement approach and explain what are the preconditions for its application. After that, in Sec. 3 we consider the infinite symbolic sequence adding scheme and its recursive definition by some

operators in the space of admissible symbolic sequences. Based on these operators we review in Sec. 4 the results obtained by Leonov regarding the period-adding structure. Eventually, in Sec. 5 we demonstrate that the application of the map replacement approach can be considered as a kind of topology-preserving mapping in the parameter space, explaining the self-similarity of the period-adding structure.

2. Basic Approach

In order to explain the basic idea of the map replacement approach, let us consider the general discontinuous piecewise-linear map defined by

$$x_{n+1} = f(x_n) = \begin{cases} f_{\mathcal{L}}(x_n) = a_\ell x_n + \mu_\ell & \text{if } x_n < 0 \\ f_{\mathcal{R}}(x_n) = a_r x_n + \mu_r & \text{if } x_n > 0 \end{cases} \tag{1}$$

which was also used in the original works [Leonov, 1959, 1960a, 1960b]. The main advantage of map (1) is that all four parameters are independent from each other. This property is crucial for the application of the map replacement approach. One further advantage of map (1) is the symmetry property

$$f(x, a_\ell, \mu_\ell, a_r, \mu_r) = -f(-x, a_r, -\mu_r, a_\ell, -\mu_\ell) \tag{2}$$

which simplifies the calculation due to the possibility of exchanging the symbols $\mathcal{L}$ and $\mathcal{R}$.

One obvious disadvantage of the general map (1) is that its parameter space is four-dimensional and hence is not easy to visualize. Therefore, we will additionally consider in the following the map with only two parameters given by

$$x_{n+1} = \begin{cases} ax_n + \mu + 1 & \text{if } x_n < 0 \\ ax_n + \mu - 1 & \text{if } x_n > 0 \end{cases} \tag{3}$$

which represents a well-known model of an electronic circuit, namely a Σ/Δ modulator. This model has been already intensively investigated by many authors (see for instance [Gray, 1987; Feely & Chua, 1991; Feely, 1992; Reiss & Sandler, 2001; Jacomet *et al.*, 2004; Coutinho *et al.*, 2006]). In this way, to keep the generality we will perform all calculation steps for the general map (1) and after that transfer the obtained results to the map (3) using the substitution

$$a_\ell = a, \quad a_r = a, \quad \mu_\ell = \mu + 1, \quad \mu_r = \mu - 1 \tag{4}$$

Note that in an analogous way all results obtained for map (1) can be transferred to any other piecewise-linear 1D map.

It is in the meanwhile well-known that when dealing with periodic orbits of such maps a symbolic description is useful. So, let σ be a symbolic sequence consisting of the letters $\sigma_i \in \{\mathcal{L}, \mathcal{R}\}$ (as usual, we write $\mathcal{L}$ for a point $x < 0$ and $\mathcal{R}$ for a point $x > 0$) corresponding to one period of a periodic orbit, which we denote by O_σ. If two sequences σ and σ' are identical up to a cyclic shift (we express that by $\sigma \equiv \sigma'$), they correspond to the same periodic orbit. Obviously, a period-n orbit O_σ of map (1) is related with fixed points of the nth iterated function $f_\sigma(x) = f_{\sigma_{n-1}} \circ \cdots \circ f_{\sigma_0}(x)$ with $n = |\sigma|$.

Let us consider the most simple case investigated also in the original works by Leonov, namely the border-collision bifurcations.[1] Proceeding in this way, let O_σ be a periodic orbit of map (1) undergoing two border-collision bifurcations. One of these bifurcations is defined by the collision of a specific point x_i^σ of the orbit with the boundary from the left side and the other one by a collision of another specific point x_j^σ of the orbit with the boundary from the right side. We denote the parameter subspace corresponding to these two bifurcations by $\xi_\sigma^{\ell,i}$ and $\xi_\sigma^{r,j}$, respectively, and use in the following the shorter notation $\xi_\sigma^{\ell,i/r,j}$ referring to both of them.

Furthermore, let O_ρ be a periodic orbit of map (1) with the symbolic sequence ρ resulting from the sequence σ by the replacement of all letters $\mathcal{L}$ by some sequence ϖ_ℓ and all letters $\mathcal{R}$ by some sequence ϖ_r, which means by a transformation in the space of admissible sequences. To give an example, for $\sigma = \mathcal{L}\mathcal{R}^3$, $\varpi_\ell = \mathcal{L}\mathcal{R}$ and $\varpi_r = \mathcal{L}\mathcal{R}^2$ we obtain $\rho = \mathcal{L}\mathcal{R}(\mathcal{L}\mathcal{R}^2)^3$. Similarly, using the same replacement, we obtain from $\sigma = \mathcal{L}\mathcal{R}(\mathcal{L}\mathcal{R}^2)^3$ the sequence $\rho = \mathcal{L}\mathcal{R}\mathcal{L}\mathcal{R}^2(\mathcal{L}\mathcal{R}(\mathcal{L}\mathcal{R}^2)^2)^3$.

Now let us assume that the periodic orbit O_ρ not only exists, but also undergoes two border-collision bifurcations, one of them by collision with the boundary from the left side by the point $x_{i'}^\rho$ and the other by collision with the boundary from the right side by the point $x_{j'}^\rho$. Of course, the sequence ρ is longer than σ and it is much easier to calculate the bifurcation subspaces $\xi_\sigma^{\ell,i/r,j}$ than $\xi_\rho^{\ell,i'/r,j'}$. The goal

[1]Note that the same approach can also be used for calculation of bifurcations of different types, as far as they are caused by contacts of some (stable or unstable) periodic orbits with some boundaries in the state space. Especially, the well-known crisis bifurcation represents an example where the approach works well.

of the map replacement approach is to reduce the complexity of the calculation in the following way: at first, the simpler bifurcation subspaces $\xi_\sigma^{\ell,i/r,j}$ will be calculated and after that the bifurcation subspaces $\xi_\rho^{\ell,i'/r,j'}$ will be obtained from this result by a suitable replacement of the parameters.

To explain how the map replacement approach works, let us consider the following example. Let us calculate the border-collision bifurcation curves for the period-11 orbit $O_{\mathcal{LR}(\mathcal{LR}^2)^3}$. This orbit collides with the boundary $x = 0$ from the left side by its third point $x_2^{\mathcal{LR}(\mathcal{LR}^2)^3}$ and from the right side by its last point $x_{10}^{\mathcal{LR}(\mathcal{LR}^2)^3}$ [see Figs. 1(e) and 1(f), respectively]. Note also that thoughout this work the points of periodic orbits are numbered according to the corresponding symbolic sequences, that means, for example, the point $x_0^{\mathcal{LR}(\mathcal{LR}^2)^3}$ corresponds to the first letter $\mathcal{L}$ in the sequence $\mathcal{LR}(\mathcal{LR}^2)^3$. The point $x_2^{\mathcal{LR}(\mathcal{LR}^2)^3}$ can be calculated straight forward by the fixed point equation

$$x = f_r \circ f_\ell \circ (f_r^2 \circ f_\ell)^3(x) \tag{5}$$

The point $x_{10}^{\mathcal{LR}(\mathcal{LR}^2)^3}$ can be calculated analogously by solving the fixed point equation

$$x = (f_r \circ f_\ell \circ f_r)^3 \circ f_\ell \circ f_r(x) \tag{6}$$

Eventually, using the border-collision conditions $x_2^{\mathcal{LR}(\mathcal{LR}^2)^3} = 0$ and $x_{10}^{\mathcal{LR}(\mathcal{LR}^2)^3} = 0$ we obtain the bifurcation curves $\xi_{\mathcal{LR}(\mathcal{LR}^2)^3}^{\ell,2}$ and $\xi_{\mathcal{LR}(\mathcal{LR}^2)^3}^{r,10}$, respectively.

As one can see, this straight forward calculation is always possible but becomes more and more complicated for increasing length and complexity of the considered orbits. Therefore, let us note that the symbolic sequence $\mathcal{LR}(\mathcal{LR}^2)^3$ can also be obtained from the much more easy sequence $\mathcal{LR}^3$ by some replacement of the letters $\mathcal{L}$ and $\mathcal{R}$. The most obvious possibility for that is

$$\mathcal{L} \to \mathcal{LR}, \quad \mathcal{R} \to \mathcal{LR}^2 \tag{7}$$

However, we use a different replacement, which is given by

$$\mathcal{L} \to \mathcal{LR}, \quad \mathcal{R} \to \mathcal{RLR} \tag{8}$$

In this case, we obtain the sequence $\mathcal{LR}(\mathcal{RLR})^3$. One can easily see that both sequences $\mathcal{LR}(\mathcal{LR}^2)^3$ and $\mathcal{LR}(\mathcal{RLR})^3$ are equivalent up to a cyclic shift

$$\begin{aligned}\mathcal{LR}(\mathcal{RLR})^3 &= \mathcal{LR} \quad \mathcal{RLR} \quad \mathcal{RLR} \quad \mathcal{RLR} \\ &= \mathcal{LRR} \quad \mathcal{LRR} \quad \mathcal{LRR} \quad \mathcal{LR} \\ &= (\mathcal{LR}^2)^3\mathcal{LR} \\ &\equiv \mathcal{LR}(\mathcal{LR}^2)^3\end{aligned} \tag{9}$$

and therefore correspond to the same orbit. The reasons why we prefer to use the replacement (8) and up to which extent the seemingly equivalent replacement (7) is different from (8) with respect to the calculation of the bifurcation curves will be explained below.

As a first step, let us calculate the border-collision bifurcation curves of the orbit $O_{\mathcal{LR}^3}$ instead of $O_{\mathcal{LR}(\mathcal{LR}^2)^3}$. For this orbit it is known that it undergoes border-collision bifurcations when its first, or last, point collides with the boundary, respectively. The first point of this orbit $x_0^{\mathcal{LR}^3}$ can be calculated straight forward by solving the fixed point equation

$$x = f_r^3 \circ f_\ell(x) \tag{10}$$

which is significantly simpler than Eq. (5). From Eq. (10) we obtain:

$$x_0^{\mathcal{LR}^3} = -\frac{a_r^3\mu_\ell + (a_r^2 + a_r + 1)\mu_r}{a_r^3 a_\ell - 1} \tag{11}$$

Similarly, for the last point of the orbit $O_{\mathcal{LR}^3}$ we obtain from $x = f_r^2 \circ f_\ell \circ f_r(x)$

$$x_3^{\mathcal{LR}^3} = -\frac{a_r^2\mu_\ell + (a_r^2 a_\ell + a_r + 1)\mu_r}{a_r^3 a_\ell - 1} \tag{12}$$

Then solving the equations $x_0^{\mathcal{LR}^3} = 0$ and $x_3^{\mathcal{LR}^3} = 0$ we obtain the following border-collision bifurcation curves

$$\xi_{\mathcal{LR}^3}^{\ell,0} = \left\{ (a_\ell, a_r, \mu_\ell, \mu_r) \,\middle|\, \frac{\mu_\ell}{\mu_r} = -\frac{a_r^2 + a_r + 1}{a_r^3} \right\} \tag{13}$$

$$\xi_{\mathcal{LR}^3}^{r,3} = \left\{ (a_\ell, a_r, \mu_\ell, \mu_r) \,\middle|\, \frac{\mu_\ell}{\mu_r} = \frac{a_r^2 a_\ell + a_r + 1}{a_r^2} \right\} \tag{14}$$

The orbits at both bifurcations for the map (3) are shown in Figs. 1(a) and 1(b), respectively. As one can clearly see, Fig. 1(a) shows the situation at the border-collision $\xi_{\mathcal{LR}^3}^{\ell,0}$ where the orbit $O_{\mathcal{LR}^3}$ collides with the boundary $x = 0$ with its first point $x_0^{\mathcal{LR}^3}$. Similarly, in Fig. 1(b) the situation at the border-collision $\xi_{\mathcal{LR}^3}^{r,3}$ is shown, where the orbit collides with the boundary with its last point $x_3^{\mathcal{LR}^3}$.

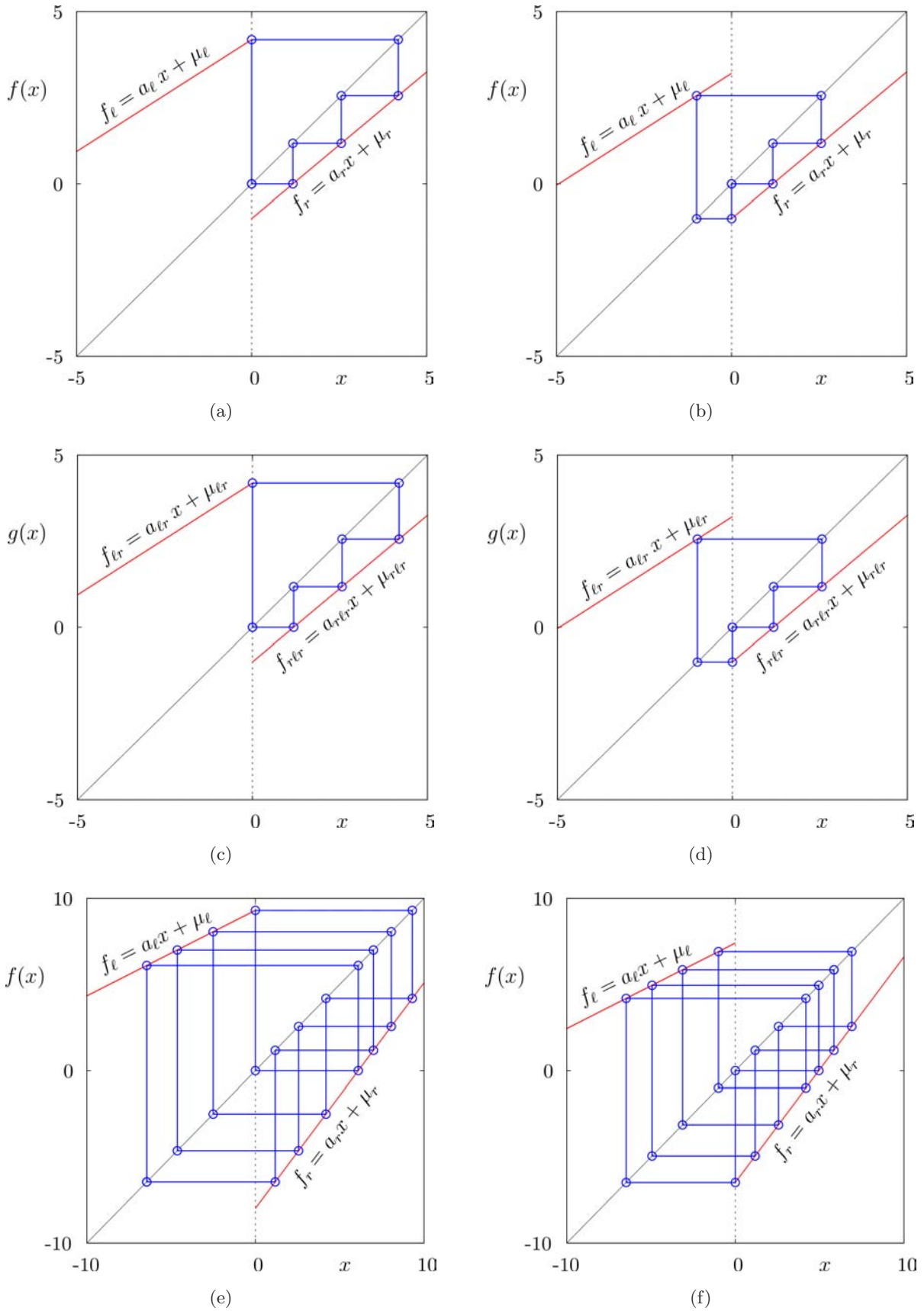

Fig. 1. Border-collision bifurcations in the original map (1) (a, b) and the composite map (17) (c, d). In (e, f) the border-collision bifurcations in the original map (1) are shown at the same parameters values as used in (c, d). For parameter values and further details see text.

So far all steps were as usual. Now let us go back to the orbit $O_{\mathcal{LR}(\mathcal{LR}^2)^3}$ and let us calculate its bifurcations from the bifurcations of the orbit $O_{\mathcal{LR}^3}$ calculated above. As already mentioned, the calculation is based on the replacement (8). According to this, let us define the following two functions:

$$f_{\ell r}(x) = f_r \circ f_\ell(x) = \underbrace{a_\ell a_r}_{a_{\ell r}} x + \underbrace{a_r \mu_\ell + \mu_r}_{\mu_{\ell r}} \tag{15}$$

$$\begin{aligned} f_{r\ell r}(x) &= f_r \circ f_\ell \circ f_r(x) \\ &= \underbrace{a_\ell a_r^2}_{a_{r\ell r}} x + \underbrace{a_r a_\ell \mu_r + a_r \mu_\ell + \mu_r}_{\mu_{r\ell r}} \end{aligned} \tag{16}$$

The most important property of the function $f(x)$ is that both iterated functions $f_{\ell r}(x)$ and $f_{r\ell r}(x)$ are linear with respect to x. As a consequence, the *composite map* defined in the following way

$$\begin{aligned} x_{n+1} &= g(x_n) \\ &= \begin{cases} f_{\ell r}(x_n) = a_{\ell r} x_n + \mu_{\ell r} & \text{if } x_n < 0 \\ f_{r\ell r}(x_n) = a_{r\ell r} x_n + \mu_{r\ell r} & \text{if } x_n > 0 \end{cases} \end{aligned} \tag{17}$$

has the same functional form as the original map (1), that means it is piecewise-linear with one point of discontinuity. The key point of the map replacement approach is that we can adjust the slopes $a_{\ell r}$, $a_{r\ell r}$, and the offsets $\mu_{\ell r}$, $\mu_{r\ell r}$, of the functions $f_{\ell r}$ and $f_{r\ell r}$ so that they are identical with the slopes a_ℓ, a_r and the offsets μ_ℓ, μ_r, of the functions f_ℓ and f_r, respectively, especially at the bifurcation values. Hence, let us consider a set of parameters $(a_{\ell r}, \mu_{\ell r}, a_{r\ell r}, \mu_{r\ell r})$ satisfying for example Eq. (14). Recall that at these parameter values the orbit $O_{\mathcal{LR}^3}$ in the original map (1) undergoes a border-collision bifurcation. Therefore, the composite map (17) shows at these parameter values the same behavior. However, recall that by definition of map (17) one step on the left side of this map represents two steps of the original map, and one step on the right side of this map represents three steps of the original map. In other words, the orbit $O_{\mathcal{LR}^3}$ of the composite map represents the orbit $O_{\mathcal{LR}(\mathcal{LR}^2)^3}$ of the original map, and therefore the orbit for which we wanted to calculate the bifurcation curves. Consequently, by substituting the parameters $(a_{\ell r}, \mu_{\ell r}, a_{r\ell r}, \mu_{r\ell r})$ in Eq. (14) we obtain the border-collision bifurcation curve for the orbit $O_{\mathcal{LR}(\mathcal{LR}^2)^3}$:

$$\xi^{r,10}_{\mathcal{LR}(\mathcal{LR}^2)^3} = \left\{ (a_\ell, a_r, \mu_\ell, \mu_r) \,\middle|\, \frac{\mu_{\ell r}}{\mu_{r\ell r}} = \frac{a_{r\ell r}^2 a_{\ell r} + a_{r\ell r} + 1}{a_{r\ell r}^2} \right\} \tag{18}$$

After that we have to insert the values of the parameters $(a_{\ell r}, \mu_{\ell r}, a_{r\ell r}, \mu_{r\ell r})$ in terms of the original parameters, as given by Eqs. (15) and (16):

$$\xi^{r,10}_{\mathcal{LR}(\mathcal{LR}^2)^3} = \left\{ (a_\ell, a_r, \mu_\ell, \mu_r) \,\middle|\, \frac{a_r \mu_\ell + \mu_r}{a_r a_\ell \mu_r + a_r \mu_\ell + \mu_r} = \frac{(a_\ell a_r^2)^2 (a_\ell a_r) + (a_\ell a_r^2) + 1}{(a_\ell a_r^2)^2} \right\} \tag{19}$$

Finally we have to resolve the last equation with respect to μ_ℓ/μ_r and obtain after some algebraic transformations the final result

$$\xi^{r,10}_{\mathcal{LR}(\mathcal{LR}^2)^3} = \left\{ (a_\ell, a_r, \mu_\ell, \mu_r) \,\middle|\, \frac{\mu_\ell}{\mu_r} = -\frac{a_\ell^2 a_r^4 + a_\ell^4 a_r^6 + a_\ell{}^3 a_r^5 + a_\ell^2 a_r^3 + a_\ell\, a_r^2 + a_\ell\, a_r + 1}{a_r \left(a_\ell^2 a_r^4 + a_\ell^3 a_r^5 + a_\ell\, a_r^2 + 1 \right)} \right\} \tag{20}$$

As one can see, the border-collision bifurcation curve $\xi^r_{\mathcal{LR}(\mathcal{LR}^2)^3}$ is now calculated using Eq. (14) which represents a much simpler bifurcation curve $\xi^r_{\mathcal{LR}^3}$ by replacing the map (1) with the composite map (17). The other border-collision bifurcation curve $\xi^\ell_{\mathcal{LR}(\mathcal{LR}^2)^3}$ can be obtained analogously, using the same replacement and Eq. (13) instead of Eq. (14). We obtain in this way

$$\begin{aligned} \xi^{\ell,2}_{\mathcal{LR}(\mathcal{LR}^2)^3} &= \left\{ (a_\ell, a_r, \mu_\ell, \mu_r) \,\middle|\, \frac{\mu_{\ell r}}{\mu_{r\ell r}} = -\frac{a_{r\ell r}^2 + a_{r\ell r} + 1}{a_{r\ell r}^3} \right\} \\ &= \left\{ (a_\ell, a_r, \mu_\ell, \mu_r) \,\middle|\, \frac{a_r \mu_\ell + \mu_r}{a_r a_\ell \mu_r + a_r \mu_\ell + \mu_r} = -\frac{(a_r^2 a_\ell)^2 + a_r^2 a_\ell + 1}{(a_r^2 a_\ell)^3} \right\} \\ &= \left\{ (a_\ell, a_r, \mu_\ell, \mu_r) \,\middle|\, \frac{\mu_\ell}{\mu_r} = -\frac{a_\ell^3 a_r^6 + a_\ell^3 a_r^5 + a_\ell^2 a_r^4 + a_\ell^2 a_r^3 + a_\ell a_r^2 + a_\ell a_r + 1}{a_r (a_\ell^3 a_r^6 + a_\ell^2 a_r^4 + a_\ell a_r^2 + 1)} \right\} \end{aligned} \tag{21}$$

To summarize, we can represent the calculation steps described above by the following replacement scheme:

$$\xi^{\ell,0/r,3}_{\mathcal{LR}^3} \xrightarrow[\substack{a_\ell \mapsto a_{\ell r} \quad a_r \mapsto a_{r\ell r} \\ \mu_\ell \mapsto \mu_{\ell r} \quad \mu_r \mapsto \mu_{r\ell r}}]{\substack{\mathcal{L} \mapsto \mathcal{LR} \\ \mathcal{R} \mapsto \mathcal{RLR}}} \xi^{\ell,2/r,10}_{\mathcal{LR}(\mathcal{LR}^2)^3} \tag{22}$$

The described procedure is illustrated in Fig. 1. As already mentioned, Figs. 1(a) and 1(b) show the orbit $O_{\mathcal{LR}^3}$ of map (1) at the bifurcations $\xi^{\ell,0}_{\mathcal{LR}^3}$ and $\xi^{r,3}_{\mathcal{LR}^3}$, respectively. Obviously, the used parameter sets

$$(a_\ell, a_r, \mu_\ell, \mu_r) = (0.65, 0.85, 4.188887, -1) \tag{23}$$

$$(a_\ell, a_r, \mu_\ell, \mu_r) = (0.65, 0.85, 3.210553, -1) \tag{24}$$

satisfy Eqs. (13) and (14), respectively. Then we set the parameters of the composite map (17) to the same values:

$$(a_{\ell r}, a_{r\ell r}, \mu_{\ell r}, \mu_{r\ell r}) = (0.65, 0.85, 4.188887, -1) \tag{25}$$

$$(a_{\ell r}, a_{r\ell r}, \mu_{\ell r}, \mu_{r\ell r}) = (0.65, 0.85, 3.210553, -1) \tag{26}$$

Finally, we solve the expressions for the parameters of the composite map (17) defined by Eqs. (15) and (16) with respect to the parameters of the original map (1) and get:

$$a_\ell = \frac{a^2_{\ell r}}{a_{r\ell r}}, \quad a_r = \frac{a_{r\ell r}}{a_{\ell r}}, \qquad \mu_\ell = \frac{a_{\ell r}\mu_{\ell r} - \mu_{r\ell r} + \mu_{\ell r}}{a_{r\ell r}}, \quad \mu_r = \frac{\mu_{r\ell r} - \mu_{\ell r}}{a_{\ell r}} \tag{27}$$

Inserting the parameter sets (25) and (26) in Eqs. (27) we obtain the following parameter sets

$$(a_\ell, a_r, \mu_\ell, \mu_r) = (0.497059, 1.307692, 9.307838, -7.982902) \tag{28}$$

$$(a_\ell, a_r, \mu_\ell, \mu_r) = (0.497059, 1.307692, 7.408722, -6.477775) \tag{29}$$

where the composite map (17) coincides with the original map (1) evaluated at the parameter sets (23) and (24), respectively, and hence shows the same behavior, as illustrated in Figs. 1(c) and 1(d). Consequently, for map (1) the parameter sets (28) and (29) lead to the situations where the orbit $O_{\mathcal{LR}(\mathcal{LR}^2)^3}$ undergoes the bifurcations $\xi^{\ell,2}_{\mathcal{LR}(\mathcal{LR}^2)^3}$ and $\xi^{r,10}_{\mathcal{LR}(\mathcal{LR}^2)^3}$, respectively, as shown in Figs. 1(e) and 1(f).

The bifurcation curves of the orbits $O_{\mathcal{LR}^3}$ and $O_{\mathcal{LR}(\mathcal{LR}^2)^3}$ for map (3) are shown in Fig. 2(a). The depicted curves are obtained from Eqs. (13), (14), (20) and (21) using substitution (4). As one can see, the shapes of the regions of existence $\mathcal{P}_{\mathcal{LR}^3}$ and $\mathcal{P}_{\mathcal{LR}(\mathcal{LR}^2)^3}$ are similar: both regions originate from the same point $a = 0$, $\mu = 1$; then they collapse to singular points at the line $a = 1$ where both orbits become unstable, and for increasing a their boundaries tend pairwise asymptotically to each other and converge to the points $a = +\infty$, $\mu = \pm 1$. This similarity is due to the fact that both orbits $O_{\mathcal{LR}^3}$ and $O_{\mathcal{LR}(\mathcal{LR}^2)^3}$ we considered are involved in the same period-adding structure. For the description of this structure, the map replacement approach is very useful, as we will see later.

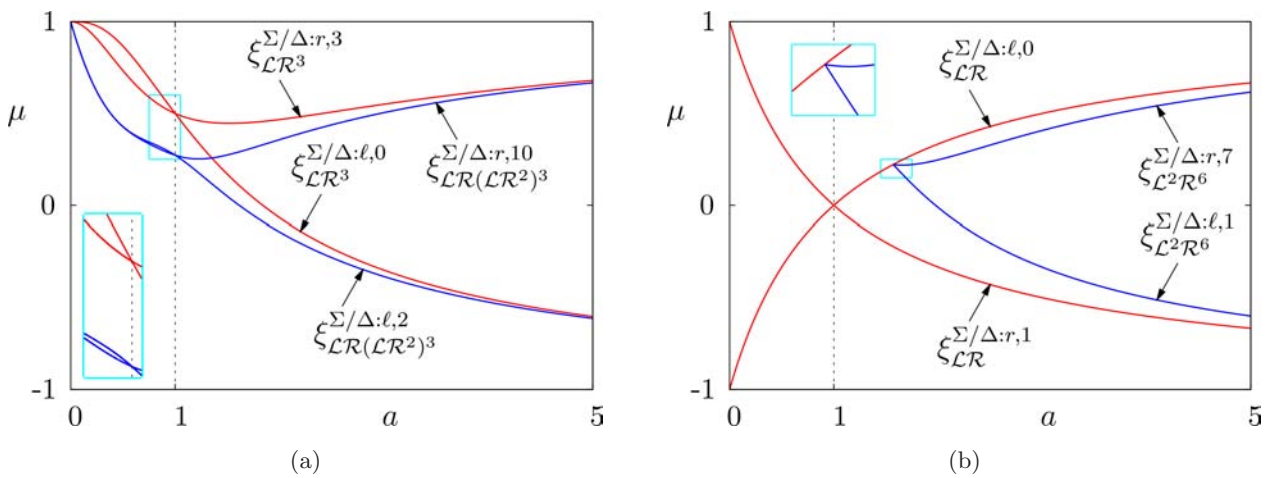

Fig. 2. Bifurcation curves in map (3) calculated by map replacement approach. (a) Bifurcations of the period-11 orbit $O_{\mathcal{LR}(\mathcal{LR}^2)^3}$ calculated starting from the bifurcations of the period-4 orbit $O_{\mathcal{LR}^3}$. (b) Bifurcations of the period-8 orbit $O_{\mathcal{L}^2\mathcal{R}^6}$ calculated starting from the bifurcations of the period-2 orbit $O_{\mathcal{LR}}$. Insets show the marked rectangles enlarged.

To obtain this replacement of the coefficients, let us first consider a symbolic sequence $\varpi = \varpi_1\varpi_2\cdots\varpi_{n-1}\varpi_n$ with period $n = |\varpi|$. Since f is a piecewise-linear function, the iterated function $f^{[n]}(x)$ is piecewise-linear too. Since f is defined on two partitions, the maximum number of partitions for $f^{[n]}$ is 2^n. In the case that the function f has a n-periodic orbit O_ϖ, the iterated function $f^{[n]}$ has n fixed points corresponding to the specific points of O_ϖ. Due to the linearity of the function $f^{[n]}(x)$ in each partition, it is clear that each of these fixed points is located in a different partition.

Let us denote by $\overleftarrow{\varpi}^n$ a symbolic sequence which results from ϖ by a cyclic shift by n. For example, $\overleftarrow{\varpi}^0 = \varpi$, $\overleftarrow{\varpi}^1 = \varpi_2\varpi_3\cdots\varpi_n\varpi_1$, and $\overleftarrow{\varpi}^2 = \varpi_3\varpi_4\cdots\varpi_1\varpi_2$. Then the fixed points of $f^{[n]}$ mentioned above are located in the partitions given by the n linear functions $f_{\overleftarrow{\varpi}^i}(x)$ with $i = 0,\ldots,n-1$. Recall that according to our notation the function $f_{\overleftarrow{\varpi}^i}(x)$ represents a subsequent application of the functions $f_{\mathcal{L}}(x)$ and $f_{\mathcal{R}}(x)$ according to the sequence $\overleftarrow{\varpi}^i$. As a consequence, when dealing with a border-collision bifurcation of the orbit O_ϖ whereby a specific point (say, the kth point) collides with the boundary $x = 0$, only one linear function $f_{\overleftarrow{\varpi}^k}(x)$ for this specific k needs to be considered.

As a matter of fact, the procedure described above can significantly simplify the calculations. Therefore, the question arises how generic is this procedure. More precisely, if a (complex) symbolic sequence ρ is given, the question is how to determine a simpler sequence σ so that the bifurcations of the orbit O_ρ can be calculated from the bifurcations of the orbit O_σ using some replacement? If a pair of sequences σ and ρ are given, so that there exists a replacement leading from the sequence σ to the sequence ρ, is it always guaranteed that the bifurcation curves for O_ρ can be calculated using the bifurcation curves for O_σ as it was done above?

Let us summarize the notation used in the following. Starting from the bifurcation curves for the orbit O_σ we will calculate the bifurcation curves for the orbit O_ρ by replacement of the parameters in the equations for the bifurcation curves for O_σ. So, the sequence $\sigma = \sigma_0\sigma_1\sigma_2\ldots\sigma_{n-1}$ with the letters $\sigma_i \in \{\mathcal{L},\mathcal{R}\}\, i = 1,\ldots,n, n = |\sigma|$ will be denoted as a *starting sequence* for the replacement. The letters σ_i in the sequence σ will be replaced by the symbolic sequences ϖ_ℓ and ϖ_r which we denote as *syllables*. Obviously, after each $\mathcal{L}$ in σ is replaced by ϖ_ℓ and each $\mathcal{R}$ by ϖ_r, the resulting sequence (also denoted as a *target sequence*) ρ can be written as

$$\rho = \varpi_0\varpi_1\varpi_2\cdots\varpi_{n-1} \quad \text{with} \quad \varpi_i = \begin{cases} \varpi_\ell & \text{if } \sigma_i = \mathcal{L} \\ \varpi_r & \text{if } \sigma_i = \mathcal{R} \end{cases} \tag{30}$$

In the example discussed above the starting sequence is $\sigma = \mathcal{L}\mathcal{R}^3$, the target sequence is $\rho = \mathcal{L}\mathcal{R}(\mathcal{L}\mathcal{R}^2)^3$, and the syllables used for the replacement are $\varpi_\ell = \mathcal{L}\mathcal{R}$, $\varpi_r = \mathcal{R}\mathcal{L}\mathcal{R}$. For the sake of clarity, the replacements $\mathcal{L} \to \varpi_\ell$ and $\mathcal{R} \to \varpi_r$ will be denoted as left and right replacements, respectively. Furthermore, we denote a replacement $(\mathcal{L} \to \varpi_\ell, \mathcal{R} \to \varpi_r)$ as *admissible*, if the calculation of the bifurcation curves for the orbit O_ρ using the replacement of the parameters (slopes and offsets) defined by the linear functions f_{ϖ_l} and f_{ϖ_r} into the expressions for the bifurcation curves of the orbit O_σ leads to a correct result. As we will see below, there are admissible and not admissible replacements.

For the calculation of border-collision bifurcation curves it is essential to know which points of the orbits O_σ and O_ρ collide with the boundary. We denote the letters corresponding to these points as *colliding letters* and underline them. In the example discussed above we have

$$\sigma = \mathcal{L}\mathcal{R}^3 = \underline{\mathcal{L}}\mathcal{R}\mathcal{R}\underline{\mathcal{R}} \quad \text{and} \quad \rho = \mathcal{L}\mathcal{R}(\mathcal{R}\mathcal{L}\mathcal{R})^3 = \underline{\mathcal{L}}\mathcal{R}\,\mathcal{R}\mathcal{L}\mathcal{R}\,\mathcal{R}\mathcal{L}\mathcal{R}\,\underline{\mathcal{R}}\mathcal{L}\mathcal{R} \tag{31}$$

In the following, we assume that each periodic orbit we consider undergoes one border-collision bifurcation where it collides with the boundary from the left side (left bifurcation), and one bifurcation where it collides from the right side (right bifurcation). Hence, each symbolic sequence corresponding to a periodic orbit of map (1) contains one colliding letter $\mathcal{L}$ and one colliding letter $\mathcal{R}$.

Which letters are colliding in a particular symbolic sequence, depends on the mechanism leading periodic orbits to emerge. Regarding orbits of type $\mathcal{L}\mathcal{R}^n$ in 1D piecewise-linear maps like (1), it is known in the case that both slopes are positive, the system function forms some kind of channel with the bisecting line and the colliding letters are the (only) symbol $\mathcal{L}$ and the last symbol $\mathcal{R}$. By contrast, in the case that one slope is positive and the other one is negative (and both offsets are positive), the system function forms some kind of swirl around an unstable fixed point, and the colliding letter $\mathcal{R}$ is not the last but the second to last one.

All the results presented below are based on the following conjecture:

> *The replacement* $\mathcal{L} \to \varpi_\ell$ *and* $\mathcal{R} \to \varpi_r$ *is admissible for the calculation of the left (resp. right) bifurcation iff the syllable* ϖ_ℓ *(resp.* ϖ_r*) in the sequences* ρ *which correspond to the colliding letter* $\mathcal{L}$ *(resp.* $\mathcal{R}$*) in* σ*, starts with the colliding letter* $\mathcal{L}$ *(resp.* $\mathcal{R}$*).*

It becomes immediately clear that if a replacement is admissible for the calculation of the left bifurcation, then ϖ_ℓ starts with $\mathcal{L}$. Note that in this case nothing is said about ϖ_r: it may start with $\mathcal{R}$ or with $\mathcal{L}$. Similarly, if a replacement is admissible for the calculation of the right bifurcation, then ϖ_r starts with $\mathcal{R}$, whereas ϖ_ℓ may start with an arbitrary letter.

Note that the symbolic replacement technique we use in this work is closely related to the symbolic *inflation* technique described in [Procaccia *et al.*, 1987]. However, the aims of both works are different. In the cited work this technique is used within the context of renormalization group theory, whereas we are calculating bifurcation curves. Since the maps considered in [Procaccia *et al.*, 1987] are piecewise-nonlinear and hence do not preserve their functional form under iterated application, the calculation of bifurcation curves by map replacements is not possible for these maps.

Let us now turn back to the example $\sigma = \mathcal{L}\mathcal{R}^3$, $\rho = \mathcal{L}\mathcal{R}(\mathcal{L}\mathcal{R}^2)^3$ discussed above and compare the replacement (8) we used, with the seemingly "more obvious" but unfortunately not admissible replacement (7). For the replacement (8) the following scheme

$$\sigma = \underline{\mathcal{L}}\mathcal{R}\mathcal{R}\underline{\mathcal{R}} \xrightarrow{\tau := \begin{cases} \mathcal{L} \mapsto \mathcal{L}\mathcal{R} \\ \mathcal{R} \mapsto \mathcal{R}\mathcal{L}\mathcal{R} \end{cases}} \rho$$

$$= \overbrace{\underline{\mathcal{L}}\mathcal{R}}^{\tau(\sigma_0)}\ \overbrace{\mathcal{R}\mathcal{L}\mathcal{R}}^{\tau(\sigma_1)}\ \overbrace{\mathcal{R}\mathcal{L}\mathcal{R}}^{\tau(\sigma_2)}\ \overbrace{\underline{\mathcal{R}}\mathcal{L}\mathcal{R}}^{\tau(\sigma_3)} \tag{32}$$

confirms that it is admissible both for the calculation of the left and of the right bifurcations. Indeed, the colliding letter $\sigma_0 = \mathcal{L}$ is mapped by (8) onto the syllable $\tau(\sigma_0) = \mathcal{L}\mathcal{R}$ where the first letter is in fact the colliding letter $\mathcal{L}$ of the sequence ρ. Similarly, the colliding letter $\sigma_3 = \mathcal{R}$ is mapped onto the syllable $\tau(\sigma_3) = \mathcal{R}\mathcal{L}\mathcal{R}$ where the first letter is the colliding letter $\mathcal{R}$ of the sequence ρ.

By contrast, the replacement (7) cannot be used neither for the calculation of the left nor of the right bifurcation. It is obvious that it is not applicable for the calculation of the right bifurcation since the syllable ϖ_r starts with $\mathcal{L}$ and not with $\mathcal{R}$. Furthermore, it is also not admissible for the calculation of the left bifurcation, since according to this replacement the colliding letter $\sigma_0 = \mathcal{L}$ will be mapped onto the syllable $\tau(\sigma_0) = \mathcal{L}\mathcal{R}$ where the first letter is now not the colliding one, as illustrated by the following scheme:

$$\sigma = \underline{\mathcal{L}}\mathcal{R}\mathcal{R}\underline{\mathcal{R}} \xrightarrow{\tau := \begin{cases} \mathcal{L} \mapsto \mathcal{L}\mathcal{R} \\ \mathcal{R} \mapsto \mathcal{L}\mathcal{R}^2 \end{cases}} \rho$$

$$= \overbrace{\mathcal{L}\mathcal{R}}^{\tau(\sigma_0)}\ \overbrace{\underline{\mathcal{L}}\mathcal{R}\mathcal{R}}^{\tau(\sigma_1)}\ \overbrace{\mathcal{L}\mathcal{R}\mathcal{R}}^{\tau(\sigma_2)}\ \overbrace{\mathcal{L}\mathcal{R}\underline{\mathcal{R}}}^{\tau(\sigma_3)} \tag{33}$$

Now let us consider a slightly more sophisticated example and calculate the bifurcation curves for the period-8 orbit O_ρ with $\rho = \mathcal{L}^2\mathcal{R}^6$. As the starting orbit we will use the period-2 orbit O_σ with $\sigma = \mathcal{L}\mathcal{R}$ (the reasons why we use this orbit are explained below). To find an admissible replacement for this calculation, we have to take into account that the colliding letters in the sequence $\mathcal{L}^2\mathcal{R}^6$ are the second $\mathcal{L}$ and the last $\mathcal{R}$. Hence, we have to split the sequence $\mathcal{L}^2\mathcal{R}^6$ (cyclically shifted in an appropriate way) in two syllables ϖ_ℓ, ϖ_r so that at least one of them starts with a colliding letter:

$$\mathcal{L}\underline{\mathcal{L}}\mathcal{R}\mathcal{R}\mathcal{R}\mathcal{R}\underline{\mathcal{R}} \equiv \varpi_\ell\varpi_r \tag{34}$$

As one can see, there are several possibilities for that. Especially, for the calculation of the left bifurcation of the orbit $O_{\mathcal{L}^2\mathcal{R}^6}$ we can use any of the following replacements:

$$\sigma = \underline{\mathcal{L}}\mathcal{R} \xrightarrow{\tau := \begin{cases} \mathcal{L} \mapsto \mathcal{L} \\ \mathcal{R} \mapsto \mathcal{R}\mathcal{R}\mathcal{R}\mathcal{R}\mathcal{R}\mathcal{L} \end{cases}} \rho = \overbrace{\underline{\mathcal{L}}}^{\tau(\sigma_0)}\ \overbrace{\mathcal{R}\mathcal{R}\mathcal{R}\mathcal{R}\mathcal{R}\mathcal{L}}^{\tau(\sigma_1)} \tag{35}$$

$$\sigma = \underline{\mathcal{L}}\mathcal{R} \xrightarrow{\tau := \begin{cases} \mathcal{L} \mapsto \mathcal{L}\mathcal{R} \\ \mathcal{R} \mapsto \mathcal{R}\mathcal{R}\mathcal{R}\mathcal{R}\mathcal{L} \end{cases}} \rho = \overbrace{\underline{\mathcal{L}}\mathcal{R}}^{\tau(\sigma_0)}\ \overbrace{\mathcal{R}\mathcal{R}\mathcal{R}\mathcal{R}\mathcal{L}}^{\tau(\sigma_1)} \tag{36}$$

$$\sigma = \underline{\mathcal{L}}\mathcal{R} \xrightarrow{\tau := \begin{cases} \mathcal{L} \mapsto \mathcal{L}\mathcal{R}\mathcal{R} \\ \mathcal{R} \mapsto \mathcal{R}\mathcal{R}\mathcal{R}\mathcal{L} \end{cases}} \rho = \overbrace{\underline{\mathcal{L}}\mathcal{R}\mathcal{R}}^{\tau(\sigma_0)}\ \overbrace{\mathcal{R}\mathcal{R}\mathcal{R}\mathcal{L}}^{\tau(\sigma_1)} \tag{37}$$

$$\sigma = \underline{\mathcal{L}}\mathcal{R} \xrightarrow{\tau:=\begin{cases}\mathcal{L}\mapsto\mathcal{L}\mathcal{R}\mathcal{R}\mathcal{R}\\ \mathcal{R}\mapsto\mathcal{R}\mathcal{R}\mathcal{R}\mathcal{L}\end{cases}} \rho = \overbrace{\underline{\mathcal{L}}\mathcal{R}\mathcal{R}\mathcal{R}}^{\tau(\sigma_0)}\ \overbrace{\mathcal{R}\mathcal{R}\mathcal{R}\mathcal{L}}^{\tau(\sigma_1)} \tag{38}$$

$$\sigma = \underline{\mathcal{L}}\mathcal{R} \xrightarrow{\tau:=\begin{cases}\mathcal{L}\mapsto\mathcal{L}\mathcal{R}\mathcal{R}\mathcal{R}\mathcal{R}\\ \mathcal{R}\mapsto\mathcal{R}\mathcal{R}\mathcal{L}\end{cases}} \rho = \overbrace{\underline{\mathcal{L}}\mathcal{R}\mathcal{R}\mathcal{R}\mathcal{R}}^{\tau(\sigma_0)}\ \overbrace{\mathcal{R}\mathcal{R}\mathcal{L}}^{\tau(\sigma_1)} \tag{39}$$

$$\sigma = \underline{\mathcal{L}}\mathcal{R} \xrightarrow{\tau:=\begin{cases}\mathcal{L}\mapsto\mathcal{L}\mathcal{R}\mathcal{R}\mathcal{R}\mathcal{R}\mathcal{R}\\ \mathcal{R}\mapsto\mathcal{R}\mathcal{L}\end{cases}} \rho = \overbrace{\underline{\mathcal{L}}\mathcal{R}\mathcal{R}\mathcal{R}\mathcal{R}\mathcal{R}}^{\tau(\sigma_0)}\ \overbrace{\mathcal{R}\mathcal{L}}^{\tau(\sigma_1)} \tag{40}$$

$$\sigma = \underline{\mathcal{L}}\mathcal{R} \xrightarrow{\tau:=\begin{cases}\mathcal{L}\mapsto\mathcal{L}\mathcal{R}\mathcal{R}\mathcal{R}\mathcal{R}\mathcal{R}\mathcal{R}\\ \mathcal{R}\mapsto\mathcal{L}\end{cases}} \rho = \overbrace{\underline{\mathcal{L}}\mathcal{R}\mathcal{R}\mathcal{R}\mathcal{R}\mathcal{R}\mathcal{R}}^{\tau(\sigma_0)}\ \overbrace{\mathcal{L}}^{\tau(\sigma_1)} \tag{41}$$

Similarly, for the calculation of the right bifurcation the following replacements are admissible:

$$\sigma = \mathcal{L}\underline{\mathcal{R}} \xrightarrow{\tau:=\begin{cases}\mathcal{L}\mapsto\mathcal{L}\mathcal{L}\mathcal{R}\mathcal{R}\mathcal{R}\mathcal{R}\\ \mathcal{R}\mapsto\mathcal{R}\end{cases}} \rho = \overbrace{\mathcal{L}\mathcal{L}\mathcal{R}\mathcal{R}\mathcal{R}\mathcal{R}}^{\tau(\sigma_0)}\ \overbrace{\underline{\mathcal{R}}}^{\tau(\sigma_1)} \tag{42}$$

$$\sigma = \mathcal{L}\underline{\mathcal{R}} \xrightarrow{\tau:=\begin{cases}\mathcal{L}\mapsto\mathcal{L}\mathcal{R}\mathcal{R}\mathcal{R}\mathcal{R}\\ \mathcal{R}\mapsto\mathcal{R}\mathcal{L}\end{cases}} \rho = \overbrace{\mathcal{L}\mathcal{R}\mathcal{R}\mathcal{R}\mathcal{R}}^{\tau(\sigma_0)}\ \overbrace{\underline{\mathcal{R}}\mathcal{L}}^{\tau(\sigma_1)} \tag{43}$$

$$\sigma = \mathcal{L}\underline{\mathcal{R}} \xrightarrow{\tau:=\begin{cases}\mathcal{L}\mapsto\mathcal{R}\mathcal{R}\mathcal{R}\mathcal{R}\\ \mathcal{R}\mapsto\mathcal{R}\mathcal{L}\mathcal{L}\end{cases}} \rho = \overbrace{\mathcal{R}\mathcal{R}\mathcal{R}\mathcal{R}}^{\tau(\sigma_0)}\ \overbrace{\underline{\mathcal{R}}\mathcal{L}\mathcal{L}}^{\tau(\sigma_1)} \tag{44}$$

$$\sigma = \mathcal{L}\underline{\mathcal{R}} \xrightarrow{\tau:=\begin{cases}\mathcal{L}\mapsto\mathcal{R}\mathcal{R}\mathcal{R}\\ \mathcal{R}\mapsto\mathcal{R}\mathcal{L}\mathcal{L}\mathcal{R}\end{cases}} \rho = \overbrace{\mathcal{R}\mathcal{R}\mathcal{R}}^{\tau(\sigma_0)}\ \overbrace{\underline{\mathcal{R}}\mathcal{L}\mathcal{L}\mathcal{R}}^{\tau(\sigma_1)} \tag{45}$$

$$\sigma = \mathcal{L}\underline{\mathcal{R}} \xrightarrow{\tau:=\begin{cases}\mathcal{L}\mapsto\mathcal{R}\mathcal{R}\\ \mathcal{R}\mapsto\mathcal{R}\mathcal{L}\mathcal{L}\mathcal{R}\mathcal{R}\end{cases}} \rho = \overbrace{\mathcal{R}\mathcal{R}}^{\tau(\sigma_0)}\ \overbrace{\underline{\mathcal{R}}\mathcal{L}\mathcal{L}\mathcal{R}\mathcal{R}}^{\tau(\sigma_1)} \tag{46}$$

$$\sigma = \mathcal{L}\underline{\mathcal{R}} \xrightarrow{\tau:=\begin{cases}\mathcal{L}\mapsto\mathcal{R}\mathcal{R}\\ \mathcal{R}\mapsto\mathcal{R}\mathcal{L}\mathcal{L}\mathcal{R}\mathcal{R}\mathcal{R}\end{cases}} \rho = \overbrace{\mathcal{R}\mathcal{R}}^{\tau(\sigma_0)}\ \overbrace{\underline{\mathcal{R}}\mathcal{L}\mathcal{L}\mathcal{R}\mathcal{R}\mathcal{R}}^{\tau(\sigma_1)} \tag{47}$$

$$\sigma = \mathcal{L}\underline{\mathcal{R}} \xrightarrow{\tau:=\begin{cases}\mathcal{L}\mapsto\mathcal{R}\\ \mathcal{R}\mapsto\mathcal{R}\mathcal{L}\mathcal{L}\mathcal{R}\mathcal{R}\mathcal{R}\end{cases}} \rho = \overbrace{\mathcal{R}}^{\tau(\sigma_0)}\ \overbrace{\underline{\mathcal{R}}\mathcal{L}\mathcal{L}\mathcal{R}\mathcal{R}\mathcal{R}}^{\tau(\sigma_1)} \tag{48}$$

As one can see, the replacements (40) and (43) are identical. Therefore the following calculation scheme is applicable for the calculation of both, the left and the right bifurcations of the orbit $O_{\mathcal{L}^2\mathcal{R}^6}$:

$$\xi^{\ell,0/r,1}_{\mathcal{L}\mathcal{R}} \xrightarrow[\substack{a_\ell\mapsto a_{\ell r^5} \quad a_r\mapsto a_{r\ell}\\ \mu_\ell\mapsto\mu_{\ell r^5} \quad \mu_r\mapsto\mu_{r\ell}}]{\substack{\mathcal{L}\mapsto\mathcal{L}\mathcal{R}^5\\ \mathcal{R}\mapsto\mathcal{R}\mathcal{L}}} \xi^{\ell,1/r,7}_{\mathcal{L}^2\mathcal{R}^6} \tag{49}$$

By contrast, all other replacements are admissible for the calculation of only one (either the left or the right) bifurcation. Nevertheless, there may be reasons why one could prefer to use them. To explain this, recall that the straight forward calculation of the bifurcations of the period-8 orbit $O_{\mathcal{L}^2\mathcal{R}^6}$ requires to calculate the 8th iterated of f, what we prefer to avoid. Using the map replacement approach we calculate these bifurcations using the bifurcation curves of the orbit $O_{\mathcal{L}\mathcal{R}}$ (calculated using the second iterated of f) and the parameters according to the particular replacement scheme. Using the scheme (49) we need the parameters $a_{\ell r^5}$ and $\mu_{\ell r^5}$ which are defined by the function $f_r^5 \circ f_\ell$, that means the sixth iterated of f. On the other hand, we can further reduce the complexity of the calculations using the replacements (38) and (45) which require to calculate the fourth iterated of f only. Proceeding in this way, we define the replacement parameters as follows:

$$\begin{aligned} f_{\ell r^3}(x) &= f_r^3 \circ f_\ell(x) \\ &= \underbrace{a_r^3 a_\ell}_{a_{\ell r^3}} x + \underbrace{a_r^3\mu_\ell + a_r^2\mu_r + a_r\mu_r + \mu_r}_{\mu_{\ell r^3}} \end{aligned} \tag{50}$$

$$f_{r^3\ell}(x) = f_\ell \circ f_r^3(x) = \underbrace{a_r^3 a_\ell}_{a_{r\ell^3}} x + \underbrace{a_\ell a_r^2 \mu_r + a_\ell a_r \mu_r + a_\ell \mu_r + \mu_\ell}_{\mu_{r\ell^3}} \tag{51}$$

$$f_{r^4}(x) = f_r^4(x) = \underbrace{a_r^4}_{a_{r^4}} x + \underbrace{a_r^3 \mu_r + a_r^2 \mu_r + a_r \mu_r + \mu_r}_{\mu_{r^4}} \tag{52}$$

$$f_{r\ell^2 r}(x) = f_r \circ f_\ell^2 \circ f_r(x) = \underbrace{a_r^2 a_\ell^2}_{a_{r\ell^2 r}} x + \underbrace{a_r a_\ell^2 \mu_r + a_r a_\ell \mu_\ell + a_r \mu_\ell + \mu_r}_{\mu_{r\ell^2 r}} \tag{53}$$

Now we can insert the parameters defined by Eqs. (50) and (51) into the equation for the left bifurcation of the orbit $O_{\mathcal{LR}}$ which is given by

$$\xi_{\mathcal{LR}}^{\ell,0} = \left\{ (a_\ell, a_r, \mu_\ell, \mu_r) \;\middle|\; \frac{\mu_\ell}{\mu_r} = -\frac{1}{a_r} \right\} \tag{54}$$

and the parameters defined by Eqs. (52) and (53) into the equation for the right bifurcation of the orbit $O_{\mathcal{LR}}$

$$\xi_{\mathcal{LR}}^{r,1} = \left\{ (a_\ell, a_r, \mu_\ell, \mu_r) \;\middle|\; \frac{\mu_\ell}{\mu_r} = -a_\ell \right\} \tag{55}$$

Inserting the parameters and solving the resulting expressions with respect to the original parameters we obtain:

$$\begin{aligned}
\xi_{\mathcal{L}^2\mathcal{R}^6}^{\ell,1} &= \left\{ (a_\ell, a_r, \mu_\ell, \mu_r) \;\middle|\; \frac{\mu_{\ell r^3}}{\mu_{r^3\ell}} = -\frac{1}{a_{r^3\ell}} \right\} \\
&= \left\{ (a_\ell, a_r, \mu_\ell, \mu_r) \;\middle|\; \frac{a_r^3\mu_\ell + a_r^2\mu_r + a_r\mu_r + \mu_r}{a_\ell a_r^2 \mu_r + a_\ell a_r \mu_r + a_\ell \mu_r + \mu_\ell} = -\frac{1}{a_r^3 a_\ell} \right\} \\
&= \left\{ (a_\ell, a_r, \mu_\ell, \mu_r) \;\middle|\; \frac{\mu_\ell}{\mu_r} = -\frac{a_\ell(a_r^2 + a_r^5 + a_r^4 + a_r^3 + a_r + 1)}{a_r^6 a_\ell + 1} \right\}
\end{aligned} \tag{56}$$

$$\begin{aligned}
\xi_{\mathcal{L}^2\mathcal{R}^6}^{r,7} &= \left\{ (a_\ell, a_r, \mu_\ell, \mu_r) \;\middle|\; \frac{\mu_{r^4}}{\mu_{r\ell^2 r}} = -a_{r^4} \right\} \\
&= \left\{ (a_\ell, a_r, \mu_\ell, \mu_r) \;\middle|\; \frac{a_r^3\mu_r + a_r^2\mu_r + a_r\mu_r + \mu_r}{a_r a_\ell^2 \mu_r + a_r a_\ell \mu_\ell + a_r \mu_\ell + \mu_r} = -a_r^4 \right\} \\
&= \left\{ (a_\ell, a_r, \mu_\ell, \mu_r) \;\middle|\; \frac{\mu_\ell}{\mu_r} = -\frac{a_r^5 a_\ell^2 + a_r^4 + a_r^3 + a_r^2 + a_r + 1}{a_r^5(a_\ell + 1)} \right\}
\end{aligned} \tag{57}$$

The question now arises whether $\mathcal{LR}$ is the only starting sequence which can be used for the calculation of the bifurcations of the orbit $O_{\mathcal{L}^2\mathcal{R}^6}$. Especially, it seems to be a natural way to start with the sequence $\mathcal{LR}^2$ or $\mathcal{LR}^3$ and to use the replacement $\mathcal{L} \to \mathcal{L}^2$, $\mathcal{R} \to \mathcal{R}^3$ or $\mathcal{R} \to \mathcal{R}^2$, respectively. It can be easily shown that this is not possible. For example, starting with the sequence $\mathcal{LR}^2$ and calculating the left bifurcation, we have to split the sequence $\mathcal{L}^2\mathcal{R}^6$ in the following way: $\rho = \underline{\mathcal{L}}\mathcal{R}\mathcal{R}\mathcal{R}\mathcal{R}\mathcal{R}\mathcal{L} = \varpi_\ell\varpi_r\varpi_r$. Hence, the syllable ϖ_ℓ must have the form $\mathcal{LR}^k$ for some $k = 0, 1, \ldots$. Consequently, the remaining suffix $\mathcal{R}^{6-k}\mathcal{L}$ must consist of two identical syllables ϖ_r what is obviously not possible, so the sequence $\mathcal{LR}^2$ cannot be used for the calculation of the left bifurcation. The proof for the sequence $\mathcal{LR}^3$ is analogous. When dealing with the right bifurcation, the situation is slightly different. In this case the sequence $\mathcal{L}^2\mathcal{R}^6$ must be split in the following way: $\rho = \underline{\mathcal{R}}\mathcal{L}\mathcal{L}\mathcal{R}\mathcal{R}\mathcal{R}\mathcal{R}\mathcal{R} = \varpi_r\varpi_\ell\varpi_r$. As one can see, there is exactly one possibility for this: $\varpi_\ell = \mathcal{L}^2\mathcal{R}^4$, $\varpi_r = \mathcal{R}$. Consequently, the sequence $\mathcal{LR}^2$ can be used as a starting sequence for the calculation of the right bifurcation of $O_{\mathcal{L}^2\mathcal{R}^6}$. However, the only admissible replacement $\mathcal{L} \to \mathcal{L}^2\mathcal{R}^4$, $\mathcal{R} \to \mathcal{R}$ requires to calculate the sixth iterated function $f_r^4 \circ f_\ell^2$ and has therefore no advantage compared to the way starting with the sequence $\mathcal{LR}$ described above.

The results obtained above — recalculated for map (3) by using the substitution (4) — are illustrated in Fig. 2(b). As one can see, the shapes of the regions $\mathcal{P}_{\mathcal{LR}}$ and $\mathcal{P}_{\mathcal{L}^2\mathcal{R}^6}$ are different. The

region $\mathcal{P}_{\mathcal{LR}}$ consists of two parts, one of them on the left side of the intersection point of the curves $\xi_{\mathcal{LR}}^{\Sigma/\Delta:\ell,0}$ and $\xi_{\mathcal{LR}}^{\Sigma/\Delta:r,1}$ (at $a < 1$) where the orbit $O_{\mathcal{LR}}$ is stable, and the other one on the right side of that point where $O_{\mathcal{LR}}$ is unstable. By contrast, the orbit $O_{\mathcal{L}^2\mathcal{R}^6}$ exists only on the right side of the intersection point of the curves $\xi_{\mathcal{L}^2\mathcal{R}^6}^{\Sigma/\Delta:\ell,1}$ and $\xi_{\mathcal{L}^2\mathcal{R}^6}^{\Sigma/\Delta:r,7}$ and is unstable in its complete existence region. It is also remarkable that the intersection point of the curves $\xi_{\mathcal{L}^2\mathcal{R}^6}^{\Sigma/\Delta:\ell,1}$ and $\xi_{\mathcal{L}^2\mathcal{R}^6}^{\Sigma/\Delta:r,7}$ is located at the curve $\xi_{\mathcal{LR}}^{\Sigma/\Delta:\ell,0}$. In fact, this intersection point where the region $\mathcal{P}_{\mathcal{L}^2\mathcal{R}^6}$ originates from is the intersection point of the curves $\xi_{\mathcal{LR}}^{\Sigma/\Delta:\ell,0}$ and $\xi_{\mathcal{LR}^5}^{\Sigma/\Delta:r,5}$. However, a detailed investigation of the question on how the existence regions of several periodic orbits within the chaotic domain are located with respect to each other is beyond the scope of this work, even if the map replacement approach simplifies this investigation significantly.

3. Period Adding: Symbolic Sequences

In the original work by Leonov the approach we discuss here was used for the calculation of border-collision bifurcation curves organized by the period adding structure.[2] In fact the application of the map replacement approach is not restricted to a specific bifurcation scenario or to a specific type of bifurcation. Nevertheless, the period adding structure represents an impressive example of a *recursive application* of the map replacement approach.

An example of the period adding structure in map (3) is shown in Fig. 3. The bifurcation diagram presented in Fig. 3(a) shows the well-known self-similar structure consisting of an infinite number of different periodic orbits with arbitrary high periods. The periods of these orbits are shown in Fig. 3(b). Similar results are presented in many works. However, Fig. 3(c) shows the same period diagram calculated analytically. As a matter of fact, it would be a very hard task to calculate this figure using usual straight forward techniques. By contrast, using the map replacement approach the calculation becomes a much simpler task. In the following we introduce the concept of complexity levels of periodic orbits. The complete Fig. 3(c) is produced using orbits of the first three complexity levels and — as we will see — is defined by only seven equations. Note also that a few of the numerically detected periods are not calculated analytically — as we will see, they belong to sequences with complexity levels larger than 3.

It is known that the rule describing the period-adding scenario is given by the infinite self-similar symbolic sequence adding scheme, whose first layers are presented in Fig. 4. This scheme can be seen as a symbolic representation of the Farey-tree [Farey, 1816; Lagarias & Tresser, 1995; Bai-Lin, 1989], which is a subtree of the Stern–Brocot tree [Stern, 1858; Brocot, 1861]. As one can see in Fig. 4, each sequence in the symbolic sequence adding scheme, except the one-letter-sequences $\mathcal{L}$ and $\mathcal{R}$ has two predecessors (which we call its *parent sequences*) and is formed by the concatenation of its parent sequences. Although the basic structure of the symbolic sequence adding scheme is well-known, there are several possibilities for how to define the substructures within this scheme, or in other words, how to group the sequences according to their location in the overall structure.

3.1. *Layers, generations and complexity levels*

The most obvious way to group the sequences is according to their *layers* in the symbolic sequence adding scheme. According to this idea, the one-letter-sequences $\mathcal{L}$ and $\mathcal{R}$ belong to the layer 0, the sequence $\mathcal{LR}$ belongs to the first layer, the sequences $\mathcal{LR}^2$ and $\mathcal{RL}^2$ belong to the second layer, the sequences $\mathcal{LR}^3$, $\mathcal{LRLR}^2$, $\mathcal{RL}^2\mathcal{RL}$, and $\mathcal{RL}^3$ to the third layer, and so on. It can be easily verified that for $i > 0$ in the ith layer there are 2^{i-1} sequences. However, this kind of grouping of the sequences has an obvious disadvantage, namely that sequences with similar forms, as for example, the family $\{\mathcal{LR}^n \,|\, n > 0\}$, are distributed among several layers, whereas the sequences of significantly different forms (for example, $\mathcal{LR}^4$, $\mathcal{LR}^2\mathcal{LR}^3$ and $\mathcal{LR}(\mathcal{LR}^2)^2$) belong to the same layer. To avoid this problem the sequences can be grouped according to their *generations* [Avrutin *et al.*, 2006; Avrutin & Schanz, 2008]. Following this idea, the two families $\{\mathcal{LR}^n \,|\, n > 0\}$ and $\{\mathcal{RL}^n \,|\, n > 0\}$ are said to form the first generation. Then, the two families of sequences whose both composing sequences belong to the first generation, that means $\{\mathcal{LR}^n\mathcal{LR}^{n+1} \,|\, n > 0\}$ and $\{\mathcal{RL}^n\mathcal{RL}^{n+1} \,|\, n > 0\}$ form the second generation, the families

[2]Note that neither the concept of border-collision bifurcations nor the period adding phenomenon were known at that time!

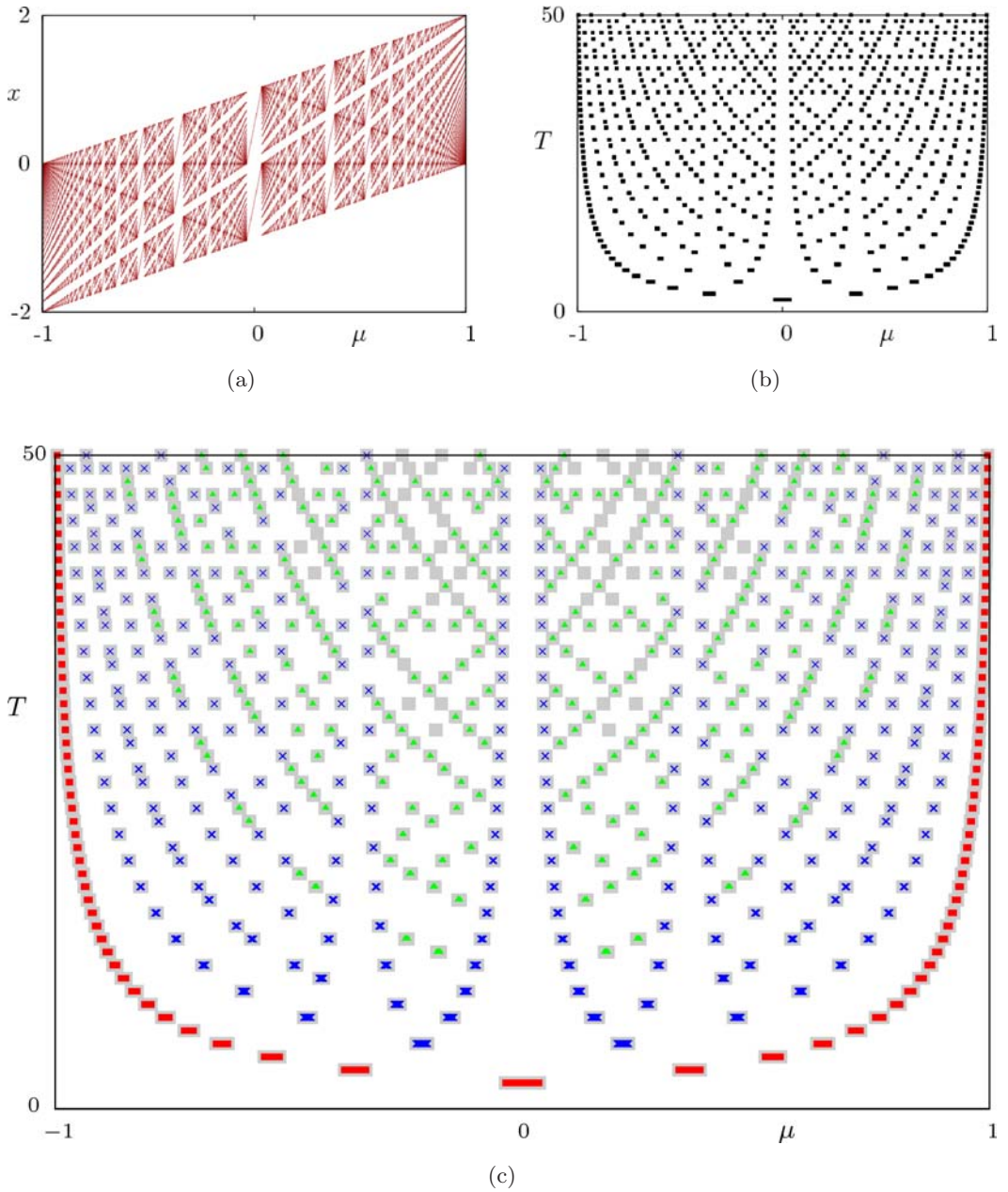

Fig. 3. Period adding structure in map (3) for $a = 0.93$: bifurcation diagram (a), period diagram calculated numerically (b) and analytically using the map replacement approach (c). In the analytically calculated period diagram periods of orbits with first, second and third complexity levels are shown with the symbols ■, × and ▲, respectively. In the background the numerical results shown in (b) are repeated as light gray rectanges.

$\{(\mathcal{LR}^n)^2\mathcal{LR}^{n+1} \,|\, n > 0\}$, $\{\mathcal{LR}^n(\mathcal{LR}^{n+1})^2 \,|\, n > 0\}$, $\{(\mathcal{RL}^n)^2\mathcal{RL}^{n+1} \,|\, n > 0\}$ and $\{\mathcal{RL}^n(\mathcal{RL}^{n+1})^2 \,|\, n > 0\}$ (for which one of the composing sequences belongs to the first generation and the other to the second generation) form the third generation, and so on. In general, the ith generations of sequences in the symbolic sequence adding scheme with $i > 2$ is formed by concatenated sequences $\sigma_1\sigma_2$, whereby the parent sequence σ_1 belongs to the generation $i - 1$. As a consequence, there are 2^{i-1} families of sequences in the ith generation. Regarding the other parent sequence σ_2 one can only say that it is one of the parent sequences of σ_1 and belongs to one of the layers $1, \ldots, i - 2$.

Note that the idea of generations seems at a first look to be motivated by the structure of the period diagram of the adding structure, as shown in Fig. 3. It is clearly visible in this figure that some periods form smooth curves, as for example, the periods of the orbits corresponding to the first

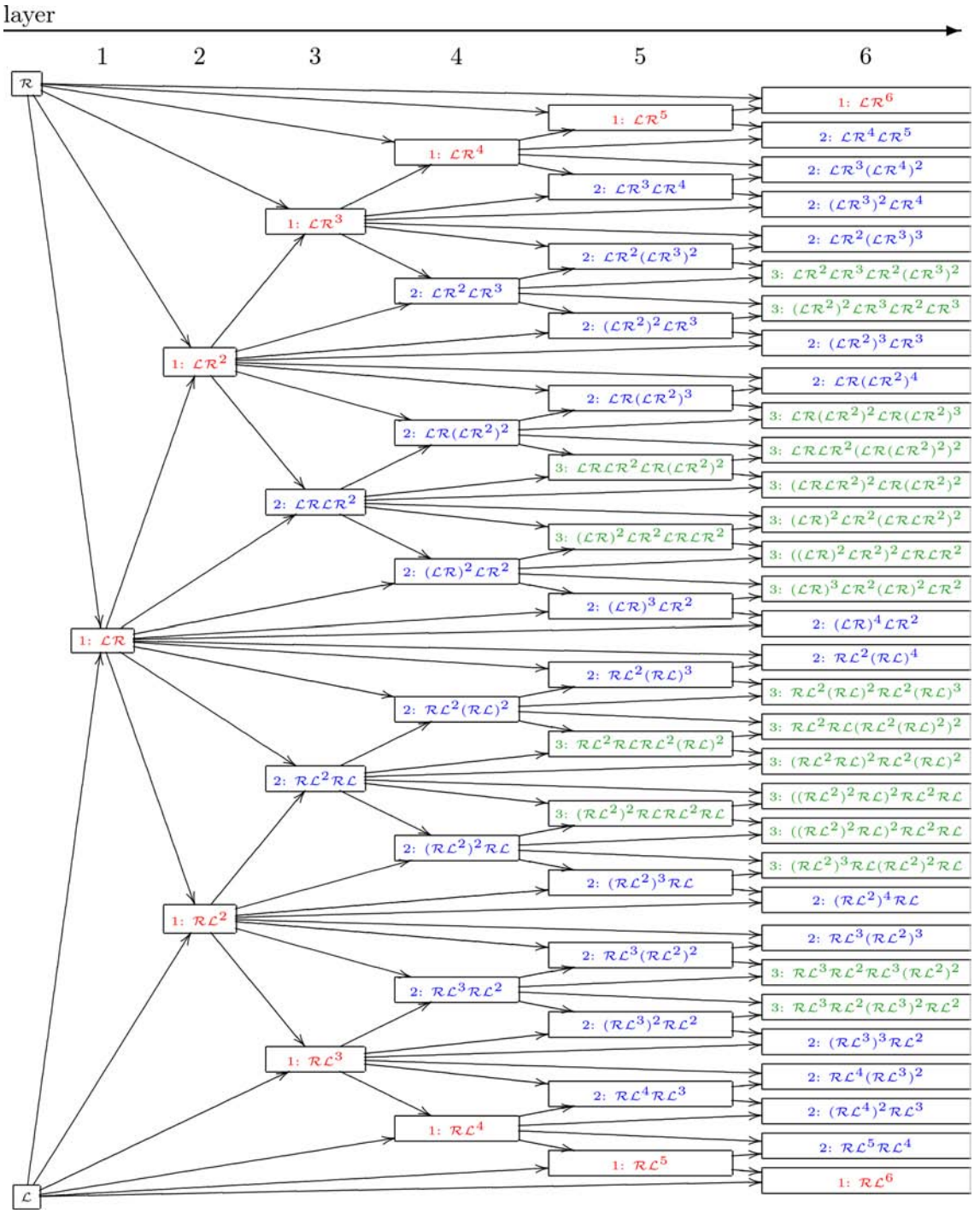

Fig. 4. First levels of the infinite symbolic sequence adding scheme. The numbers in front of the sequences refer to the complexity levels according to Leonov.

and to the second generations. However, this first impression is in general wrong, as can be seen in Fig. 5. The periods of the orbits corresponding to the fourth and to all higher generations do not form these curves. Consequently, also the generations do not represent a suitable grouping of the sequences in the adding scheme.

As a prerequisite for the recursive application of the map replacement approach, the symbolic sequences in the symbolic sequence adding scheme have to be grouped in a different way, namely according to their *complexity levels*. The first complexity level is identical with the abovementioned first generation and is given by the two

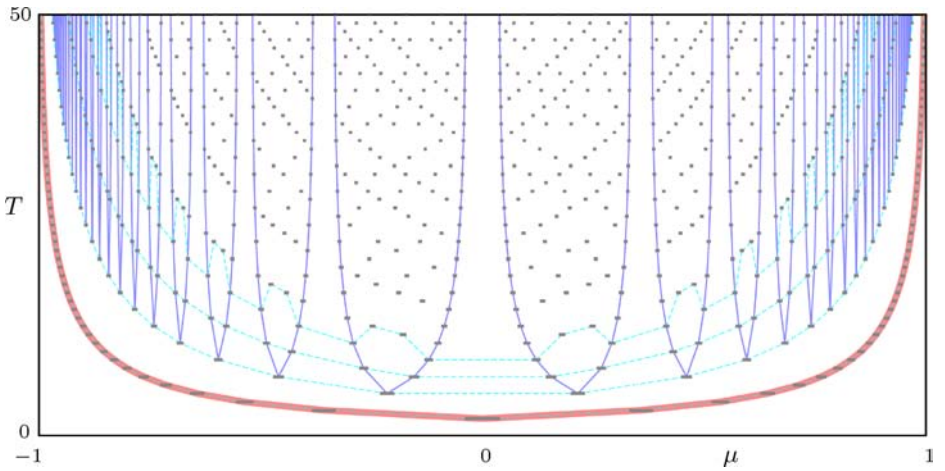

Fig. 5. Period adding structure in map (3) for $a = 0.93$ (compare Fig. 3). Red and blue lines connect the periods which belong to the same families of sequences of the first and of the second complexity levels, respectively, whereas the dashed cyan lines connect the periods of the first four generations in the symbolic sequence adding scheme.

one-parametric families:

$$\{\mathcal{L}\mathcal{R}^{n_1} \,|\, n_1 > 0\} \tag{58}$$

$$\{\mathcal{R}\mathcal{L}^{n_1} \,|\, n_1 > 0\} \tag{59}$$

The term "one-parametric" refers here to the value $n_1 > 0$ which is unspecified in case of a family of sequences but which is of course fixed for each specific sequence. The second complexity level is then given by the four two-parametric families:

$$\{\mathcal{L}\mathcal{R}^{n_2}(\mathcal{L}\mathcal{R}^{n_2+1})^{n_1} \,|\, n_1 > 0, n_2 > 0\} \tag{60}$$

$$\{\mathcal{L}\mathcal{R}^{n_2+1}(\mathcal{L}\mathcal{R}^{n_2})^{n_1} \,|\, n_1 > 0, n_2 > 0\} \tag{61}$$

$$\{\mathcal{R}\mathcal{L}^{n_2+1}(\mathcal{R}\mathcal{L}^{n_2})^{n_1} \,|\, n_1 > 0, n_2 > 0\} \tag{62}$$

$$\{\mathcal{R}\mathcal{L}^{n_2}(\mathcal{R}\mathcal{L}^{n_2+1})^{n_1} \,|\, n_1 > 0, n_2 > 0\} \tag{63}$$

In Fig. 5 this two-parametric property is clearly reflected by the U-shaped curves connecting the periods of the orbits corresponding to the second complexity level. One index belongs to each specific U-shaped curve whereas the other index runs through the periods within one U-shaped curve. A first look at these families (and all families of higher complexity level) seems to reveal that they could be obtained from the families (58) and (59) of the first complexity level using the replacements

$$\hat{\kappa}^{\ell}_{n_2} := \begin{cases} \mathcal{L} \mapsto \mathcal{L}\mathcal{R}^{n_2} \\ \mathcal{R} \mapsto \mathcal{L}\mathcal{R}^{n_2+1} \end{cases} \tag{64}$$

and

$$\hat{\kappa}^{r}_{n_2} := \begin{cases} \mathcal{L} \mapsto \mathcal{R}\mathcal{L}^{n_2+1} \\ \mathcal{R} \mapsto \mathcal{R}\mathcal{L}^{n_2} \end{cases} \tag{65}$$

However, as already pointed out in the introductory example, these replacements can be used only for the creation of the symbolic sequences but not for the calculation of the corresponding bifurcation curves. In fact, the replacements (64) and (65) do not lead to the correct colliding letters in the composite sequences and are therefore not admissible in the sense of our conjecture. By contrast, the following replacements

$$\hat{\tau}^{\ell}_{n_2} := \begin{cases} \mathcal{L} \mapsto \mathcal{L}\mathcal{R}^{n_2} \\ \mathcal{R} \mapsto \mathcal{R}\mathcal{L}\mathcal{R}^{n_2} \end{cases} \tag{66}$$

and

$$\hat{\tau}^{r}_{n_2} := \begin{cases} \mathcal{L} \mapsto \mathcal{L}\mathcal{R}\mathcal{L}^{n_2} \\ \mathcal{R} \mapsto \mathcal{R}\mathcal{L}^{n_2} \end{cases} \tag{67}$$

lead not only to the correct sequences via a cyclic shift, but are also admissible. Note that the replacements given by Eqs. (64)–(67) represent operators in the space of symbolic sequences, as described in more detail in Sec. 3.2. We want to emphasize again, that the symbolic sequences of the families (60) and (61) can be obtained from the families (58) and (59) of the first complexity level using the replacements (64) or (66), whereas the corresponding bifurcation curves can only be obtained using the replacement (66). Note that the symbolic sequences of the families (62) and (63) can be obtained from the same families (58) and (59) using the replacements (65) or (67), whereas the corresponding bifurcation curves can only be obtained using the replacement (67). For example, the family $\{\mathcal{L}\mathcal{R}^{n_2}(\mathcal{R}\mathcal{L}\mathcal{R}^{n_2})^{n_1} \,|\, n_1 > 0, n_2 > 0\}$ resulting directly from the family (58) using replacement (66)

is identical with the family (60):

$$\begin{aligned}\mathcal{LR}^{n_2}(\mathcal{RLR}^{n_2})^{n_1} &= \mathcal{LR}^{n_2}\underbrace{\mathcal{RLR}^{n_2}\cdots\mathcal{RLR}^{n_2}}_{n_1\text{ times}}\\ &= \underbrace{\mathcal{LR}^{n_2}\mathcal{R}\cdots\mathcal{LR}^{n_2}\mathcal{R}}_{n_1\text{ times}}\,\mathcal{LR}^{n_2}\\ &= (\mathcal{LR}^{n_2+1})^{n_1}\mathcal{LR}^{n_2}\\ &\equiv \mathcal{LR}^{n_2}(\mathcal{LR}^{n_2+1})^{n_1} \qquad (68)\end{aligned}$$

The proofs for the remaining three cases (61)–(63) are completely analogous.

In fact, the considerations presented above can be generalized. As a final result we obtain the following

Proposition 1. *For an arbitrary symbolic sequence σ let ρ be the symbolic sequence obtained from σ by the replacement (64) and ρ' the symbolic sequence obtained from σ by replacements (66). Then ρ and ρ' are equivalent up to a cyclic shift: $\rho \equiv \rho'$. The same holds for the replacements (65) and (67).*

A proof of this proposition is given in the Appendix. As a consequence, we have to distinguish between the following two situations. When dealing with symbolic sequences only, there is no difference whether one uses the replacements (64), (65) or (66), (67). Moreover, the replacements (64), (65) lead to a shorter and typically "better readable" representation of the resulting sequences and are preferred due to this reason. However, when calculating the bifurcation curves using the map replacement approach, only the replacements (66), (67) are admissible whereas the replacements (64), (65) are not.

Applying the replacements (66) and (67) — or equivalently (64) and (65) — on the sequences of the second complexity level given by Eqs. (60)–(63) we obtain the eight families of the third complexity level

$$\{\mathcal{LR}^{n_3}(\mathcal{LR}^{n_3+1})^{n_2}(\mathcal{LR}^{n_3}(\mathcal{LR}^{n_3+1})^{n_2+1})^{n_1}\,|\,n_1>0,n_2>0,n_3>0\} \qquad (69)$$

$$\{\mathcal{LR}^{n_3}(\mathcal{LR}^{n_3+1})^{n_2+1}(\mathcal{LR}^{n_3}(\mathcal{LR}^{n_3+1})^{n_2})^{n_1}\,|\,n_1>0,n_2>0,n_3>0\} \qquad (70)$$

$$\{\mathcal{LR}^{n_3+1}(\mathcal{LR}^{n_3})^{n_2+1}(\mathcal{LR}^{n_3+1}(\mathcal{LR}^{n_3})^{n_2})^{n_1}\,|\,n_1>0,n_2>0,n_3>0\} \qquad (71)$$

$$\{\mathcal{LR}^{n_3+1}(\mathcal{LR}^{n_3})^{n_2}(\mathcal{LR}^{n_3+1}(\mathcal{LR}^{n_3})^{n_2+1})^{n_1}\,|\,n_1>0,n_2>0,n_3>0\} \qquad (72)$$

$$\{\mathcal{RL}^{n_3+1}(\mathcal{RL}^{n_3})^{n_2}(\mathcal{RL}^{n_3+1}(\mathcal{RL}^{n_3})^{n_2+1})^{n_1}\,|\,n_1>0,n_2>0,n_3>0\} \qquad (73)$$

$$\{\mathcal{RL}^{n_3+1}(\mathcal{RL}^{n_3})^{n_2+1}(\mathcal{RL}^{n_3+1}(\mathcal{RL}^{n_3})^{n_2})^{n_1}\,|\,n_1>0,n_2>0,n_3>0\} \qquad (74)$$

$$\{\mathcal{RL}^{n_3}(\mathcal{RL}^{n_3+1})^{n_2+1}(\mathcal{RL}^{n_3}(\mathcal{RL}^{n_3+1})^{n_2})^{n_1}\,|\,n_1>0,n_2>0,n_3>0\} \qquad (75)$$

$$\{\mathcal{RL}^{n_3}(\mathcal{RL}^{n_3+1})^{n_2}(\mathcal{RL}^{n_3}(\mathcal{RL}^{n_3+1})^{n_2+1})^{n_1}\,|\,n_1>0,n_2>0,n_3>0\} \qquad (76)$$

Note that the index we use on the right-hand side of Eqs. (66) and (67) is n_3 and not n_2 to distinguish it from the index n_2 already present in Eqs. (60)–(63). Therefore, the eight families of sequences in the third complexity level are three-parametric. We also keep in mind that the families given by Eqs. (69)–(76) are written in the shorter form as they result from the replacements (64) and (65). As already mentioned, for the calculation of the corresponding bifurcation curves we have to use the admissible replacements (66) and (67).

This recursive replacement procedure will be continued *ad infinitum*. Since there are two replacements, namely Eqs. (66) and (67), the number of families of sequences will be doubled in each step. Consequently, the ith complexity level is represented by 2^i families of sequences. Moreover, since each replacement leads to one additional index n_i in the sequences, the families of the ith complexity level are i-parametric.

The grouping of the sequences in the symbolic sequence adding scheme according to their complexity levels is shown in Fig. 6. Due to the lack of space, the specific sequences are not labeled in this picture (they can be looked up in Fig. 4), instead the complete one-parametric families are marked by chains of double-stroked arrows. Recall that the families of the first complexity level are one-parametric, whereas the families of the second (respectively the third) complexity levels become one-parametric for fixed values of n_2 (respectively, n_2 and n_3).

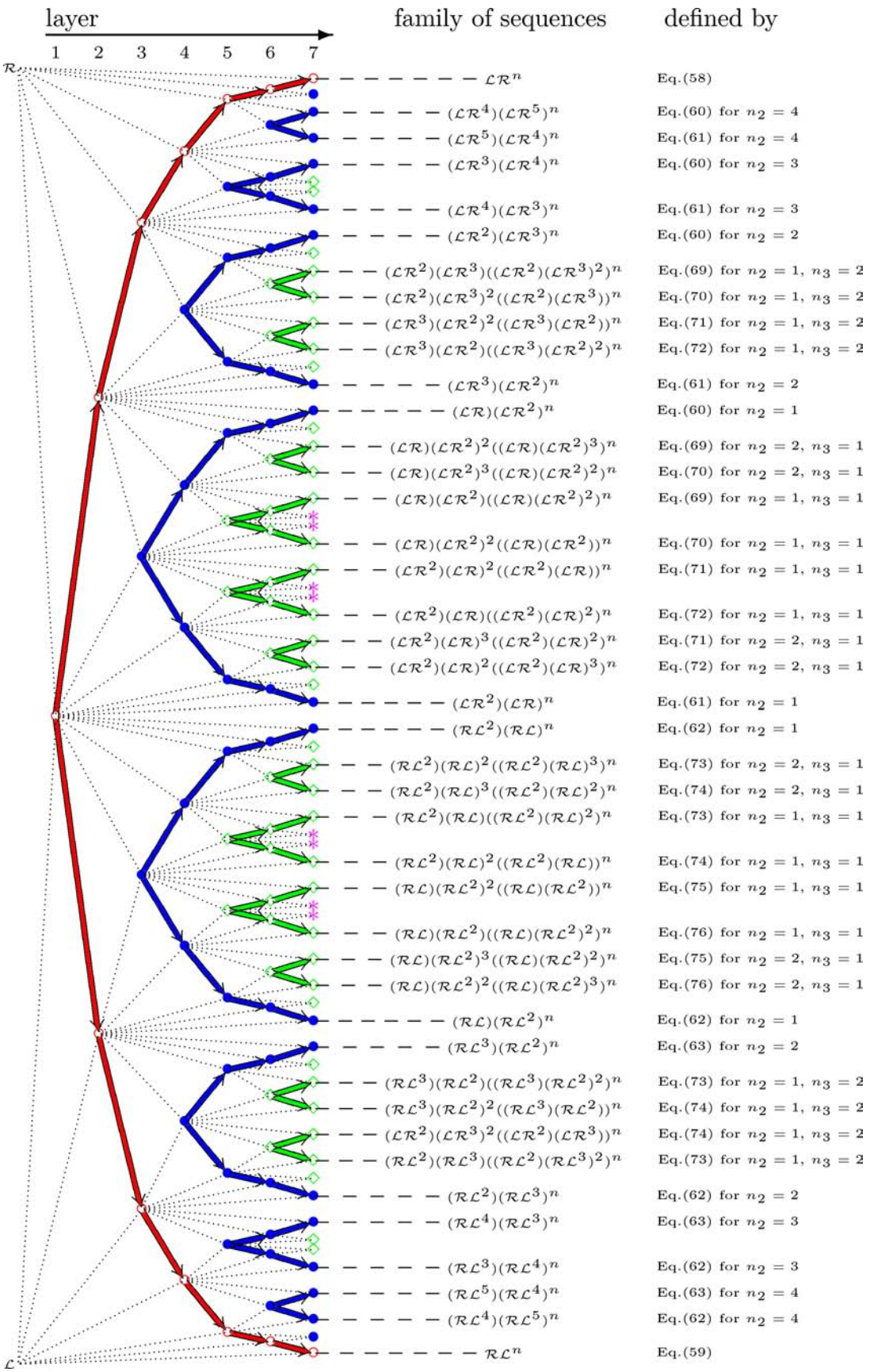

Fig. 6. Symbolic sequence adding scheme: complexity levels according to Leonov. Sequences of first, second, third and fourth complexity levels are shown as ○, ●, ◇, and ∗, respectively.

In this representation the self-similarity of the symbolic sequence adding scheme becomes clearly visible. As one can see, the structure between certain branches, for example the branches $\mathcal{LR}(\mathcal{LR}^2)^n$ and $\mathcal{LR}^2(\mathcal{LR})^n$, is topologically identical with the overall structure located between the branches $\mathcal{LR}^n$ and $\mathcal{RL}^n$. This self-similarity reflects the recursive definition of the symbolic sequence adding scheme and represents the basis for the recursive application of the map replacement approach for the calculation of the corresponding bifurcation curves.

Remarkably, the families of sequences in each complexity level are disjoint except for the case $n_1 = 1$. For $n_1 = 1$ we have pairs of families starting with sequences which are identical up to a cyclic shift. In Fig. 6 these pairs correspond to the nodes from which two double-stroked arrows originate. For example, in the second complexity level, the families given by Eqs. (60) and (61) start with the sequences

$$\mathcal{LR}^{n_2}\mathcal{LR}^{n_2+1} \equiv \mathcal{LR}^{n_2+1}\mathcal{LR}^{n_2} \tag{77}$$

Similarly, in the third complexity level, the families given by Eqs. (69) and (70) start with the sequences

$$\begin{aligned}\mathcal{LR}^{n_3}(\mathcal{LR}^{n_3+1})^{n_2}\mathcal{LR}^{n_3}(\mathcal{LR}^{n_3+1})^{n_2+1}\\ \equiv\ \mathcal{LR}^{n_3}(\mathcal{LR}^{n_3+1})^{n_2+1}\mathcal{LR}^{n_3}(\mathcal{LR}^{n_3+1})^{n_2}\end{aligned} \tag{78}$$

The reason for this ambiguity is the recursive definition of the sequences and the fact that both families of the first complexity level $\mathcal{LR}^n$ and $\mathcal{RL}^n$ start with the same sequence $\mathcal{LR}$. This ambiguity can be resolved easily defining the families in the first complexity level for $n > 1$ and treating the sequence $\mathcal{LR}$ as an exceptional case.

3.2. *Symbolic operators*

The described generation rules for the symbolic sequences with increasing complexity levels are sufficient for the application of the map replacement approach. However, for a deeper understanding of the approach it is preferable to reconsider the symbolic sequence adding scheme in some more detail. Recall that the replacements (64)–(67) represent operators in the space of symbolic sequences. In the following we use these operators for the description of the symbolic sequence adding scheme. Because this description is on a symbolic level, both pairs of operators, that means either (64), (65) or (66), (67), can be used. In the following we use the operators defined by (64) and (65), as the resulting symbolic sequences are more compact and "better readable".

As one can easily see, each of these operators $\hat{\kappa}_n^\ell$ and $\hat{\kappa}_n^r$ can be applied to a particular sequence or on a family of sequences, as for example

$$\begin{aligned}\hat{\kappa}_5^\ell(\mathcal{LR}^3) &\equiv \mathcal{LR}^5(\mathcal{LR}^6)^3\\ \hat{\kappa}_n^\ell(\mathcal{LR}^3) &\equiv \{\mathcal{LR}^n(\mathcal{LR}^{n+1})^3 \,|\, n > 0\}\\ \hat{\kappa}_5^\ell(\{\mathcal{LR}^n \,|\, n > 0\}) &\equiv \{\mathcal{LR}^5(\mathcal{LR}^6)^n \,|\, n > 0\}\\ \hat{\kappa}_{n_2}^\ell(\{\mathcal{LR}^{n_1} \,|\, n_1 > 0\}) &\equiv \{\mathcal{LR}^{n_2}(\mathcal{LR}^{n_2+1})^{n_1}\\ &\qquad |\, n_1 > 0, n_2 > 0\}\end{aligned} \tag{79}$$

Recall that the symbolic sequence adding scheme can be defined recursively. Therefore, each symbolic sequence ρ of the ith complexity level can be obtained from a sequence σ of the first complexity level by application of a sequence of operators:

$$\begin{aligned}\rho = \hat{\kappa}_{n_{i-1}}^{d_{i-1}} \circ \hat{\kappa}_{n_{i-2}}^{d_{i-2}} \circ \cdots \circ \hat{\kappa}_{n_1}^{d_1}(\sigma), \quad \text{with}\\ d_k \in \{\ell, r\},\ \ k = 1, \ldots, i-1\end{aligned} \tag{80}$$

In the following, we denote the sequence

$$\begin{aligned}\rho' = \hat{\kappa}_{n_{i-2}}^{d_{i-2}} \circ \cdots \circ \hat{\kappa}_{n_1}^{d_1}(\sigma), \quad \text{with}\\ d_k \in \{\ell, r\},\ \ k = 1, \ldots, i-2\end{aligned} \tag{81}$$

as the *first-order preimage* of ρ. Similarly, the first-order preimage of ρ' is the second-order preimage of ρ, and so on. Let us illustrate this by the following example. The sequence

$$\begin{aligned}\rho = \mathcal{RL}^3(\mathcal{RL}^2)^3(\mathcal{RL}^3(\mathcal{RL}^2)^2)^4\\ \times (\mathcal{RL}^3(\mathcal{RL}^2)^3(\mathcal{RL}^3(\mathcal{RL}^2)^2)^3)^2\end{aligned} \tag{82}$$

corresponding to a period-139 orbit, belongs to the fourth complexity level. The corresponding sequence of operators leading to ρ from a sequence of the first complexity level is given by $\hat{\kappa}_2^r \circ \hat{\kappa}_2^\ell \circ \hat{\kappa}_3^r$. This follows from the fact, that the sequence $\rho' = \mathcal{LR}^3(\mathcal{LR}^2)^4(\mathcal{LR}^3(\mathcal{LR}^2)^3)^2$ of the third complexity level is the first-order preimage of ρ. The sequence $\rho'' = \mathcal{RL}^4(\mathcal{RL}^3)^2$ of the second complexity level is the first-order preimage of ρ' and hence the second-order preimage of ρ. Finally, the sequence $\rho''' = \mathcal{LR}^2$ of the first complexity level is the third-order preimage of ρ. To demonstrate that, it is sufficient to notice that the sequence ρ consists of syllables $\mathcal{RL}^3$ and $\mathcal{RL}^2$. The operator which creates these syllables, is $\hat{\kappa}_2^r$, defined by Eq. (65). Hence, to obtain the first-order preimage of ρ we have to collapse each of these syllables to single symbols $\mathcal{L}$

and $\mathcal{R}$ as follows:

$$\begin{array}{l}\rho = \underbrace{\underbrace{\mathcal{R}}_{\mathcal{L}}\underbrace{\mathcal{L}^3}_{\mathcal{R}}(\underbrace{\mathcal{R}}_{\mathcal{L}}\underbrace{\mathcal{L}^2}_{\mathcal{R}})^3}_{\mathcal{L}\mathcal{R}^3}\ \underbrace{(\underbrace{\mathcal{R}}_{\mathcal{L}}\underbrace{\mathcal{L}^3}_{\mathcal{R}}(\underbrace{\mathcal{R}}_{\mathcal{L}}\underbrace{\mathcal{L}^2}_{\mathcal{R}})^2)^4}_{(\mathcal{L}\mathcal{R}^2)^4}\ \underbrace{(\underbrace{\mathcal{R}}_{\mathcal{L}}\underbrace{\mathcal{L}^3}_{\mathcal{R}}(\underbrace{\mathcal{R}}_{\mathcal{L}}\underbrace{\mathcal{L}^2}_{\mathcal{R}})^3(\underbrace{\mathcal{R}}_{\mathcal{L}}\underbrace{\mathcal{L}^3}_{\mathcal{R}}(\underbrace{\mathcal{R}}_{\mathcal{L}}\underbrace{\mathcal{L}^2}_{\mathcal{R}})^2)^3)^2}_{(\mathcal{L}\mathcal{R}^3(\mathcal{L}\mathcal{R}^2)^3)^2} \\ \rho' \rightarrow \end{array} \tag{83}$$

This leads us to the sequence ρ'. It consists of the syllables $\mathcal{L}\mathcal{R}^3$ and $\mathcal{L}\mathcal{R}^2$ which can be created by applying the operator $\hat{\kappa}_2^\ell$, defined by Eq. (64). We collapse them correspondingly to single symbols $\mathcal{R}$ and $\mathcal{L}$

$$\begin{array}{l}\rho' = \underbrace{\underbrace{\mathcal{L}}_{\mathcal{R}}\underbrace{\mathcal{R}^3}_{\mathcal{L}}(\underbrace{\mathcal{L}}_{\mathcal{R}}\underbrace{\mathcal{R}^2}_{\mathcal{L}})^4}_{\mathcal{R}\mathcal{L}^4}\ \underbrace{(\underbrace{\mathcal{L}}_{\mathcal{R}}\underbrace{\mathcal{R}^3}_{\mathcal{L}}(\underbrace{\mathcal{L}}_{\mathcal{R}}\underbrace{\mathcal{R}^2}_{\mathcal{L}})^3)^2}_{(\mathcal{R}\mathcal{L}^3)^2} \\ \rho'' \rightarrow \end{array} \tag{84}$$

and obtain the sequence ρ''. Eventually, the syllables $\mathcal{R}\mathcal{L}^3$ and $\mathcal{R}\mathcal{L}^4$ will be collapsed using the replacement (65) again:

$$\begin{array}{l}\rho'' = \underbrace{\underbrace{\mathcal{R}}_{\mathcal{L}}\underbrace{\mathcal{L}^4}_{\mathcal{R}}(\underbrace{\mathcal{R}}_{\mathcal{L}}\underbrace{\mathcal{L}^3}_{\mathcal{R}})^2}_{\mathcal{L}\mathcal{R}^2} \\ \rho''' \rightarrow \end{array} \tag{85}$$

The operator applied in this case is $\hat{\kappa}_3^r$. To summarize, we yield $\rho = \hat{\kappa}_2^r(\rho')$, $\rho' = \hat{\kappa}_2^\ell(\rho'')$, $\rho'' = \hat{\kappa}_3^r(\rho''')$, and therefore $\rho = \hat{\kappa}_2^r \circ \hat{\kappa}_2^\ell \circ \hat{\kappa}_3^r(\rho''')$.

Further examples for the described mechanism are shown in Fig. 7. In this figure, the symbolic sequences listed in Table 1 are labeled as σ_i, $i = 1, \ldots, 16$ and the double-stroked arrows show the paths connecting them with the sequences of the first complexity level. Obviously, each specific arrow in this figure corresponds to the application of one of the operators $\hat{\kappa}_n^\ell$, $\hat{\kappa}_n^r$ with a corresponding specific value of n. As one can see, all four sequences σ_{11}, σ_{12}, σ_{13}, σ_{14} of the fourth complexity level have the sequence σ_1, that means $\mathcal{L}\mathcal{R}$, as third-order preimage. However, the application of the operators $\hat{\kappa}_n^\ell$ and $\hat{\kappa}_n^r$ is different:

$$\sigma_{11} = \hat{\kappa}_1^\ell(\sigma_5) = \hat{\kappa}_1^\ell \circ \hat{\kappa}_1^\ell(\sigma_3) = \hat{\kappa}_1^\ell \circ \hat{\kappa}_1^\ell \circ \hat{\kappa}_1^\ell(\sigma_1) \tag{86}$$

$$\sigma_{12} = \hat{\kappa}_1^\ell(\sigma_6) = \hat{\kappa}_1^\ell \circ \hat{\kappa}_1^\ell(\sigma_4) = \hat{\kappa}_1^\ell \circ \hat{\kappa}_1^\ell \circ \hat{\kappa}_1^r(\sigma_1) \tag{87}$$

$$\sigma_{13} = \hat{\kappa}_1^\ell(\sigma_7) = \hat{\kappa}_1^\ell \circ \hat{\kappa}_1^r(\sigma_3) = \hat{\kappa}_1^\ell \circ \hat{\kappa}_1^r \circ \hat{\kappa}_1^\ell(\sigma_1) \tag{88}$$

$$\sigma_{14} = \hat{\kappa}_1^\ell(\sigma_8) = \hat{\kappa}_1^\ell \circ \hat{\kappa}_1^r(\sigma_4) = \hat{\kappa}_1^\ell \circ \hat{\kappa}_1^r \circ \hat{\kappa}_1^r(\sigma_1) \tag{89}$$

Note further that the sequences located in the upper half of the symbolic sequence adding scheme (above $\mathcal{L}\mathcal{R}$) consist of syllables of the form $\mathcal{L}\mathcal{R}^n$, while the sequences located in the lower half of the symbolic sequence adding scheme (below $\mathcal{L}\mathcal{R}$) consist of syllables of the form $\mathcal{R}\mathcal{L}^n$. As one can see, each application of the operator $\hat{\kappa}_n^\ell$ leads to a sequence located in the upper half of the symbolic sequence adding scheme, whereas each application of the operator $\hat{\kappa}_n^r$ leads to a sequence located in the lower half. Consequently, if a sequence ρ is located, for example, in the upper half of the symbolic sequence adding scheme, the preimages of ρ may be distributed among the complete symbolic sequence adding scheme and are not necessarily located in the upper half. This is illustrated in Fig. 7. The sequence σ_{15}, for example, is located in the upper half of the symbolic sequence adding scheme and consists of the syllables $\mathcal{L}\mathcal{R}$ and $\mathcal{L}\mathcal{R}^2$, whereas its preimage is located in the lower half and is given by $\sigma_{10} = \mathcal{R}\mathcal{L}^5$. Similarly, the first-order preimage of σ_{16} consists of the syllables $\mathcal{R}\mathcal{L}^2$ and $\mathcal{R}\mathcal{L}^3$, whereas the second-order preimage is $\mathcal{L}\mathcal{R}^2$.

Table 1. Abbreviations used in Fig. 7.

Label	Sequence	Level
σ_1	$\mathcal{L}\mathcal{R}$	1
σ_2	$\mathcal{L}\mathcal{R}^2$	1
σ_3	$\mathcal{L}\mathcal{R}\,\mathcal{L}\mathcal{R}^2$	2
σ_4	$\mathcal{R}\mathcal{L}^2\,\mathcal{R}\mathcal{L}$	2
σ_5	$\mathcal{L}\mathcal{R}\,\mathcal{L}\mathcal{R}^2\,\mathcal{L}\mathcal{R}\,(\mathcal{L}\mathcal{R}^2)^2$	3
σ_6	$(\mathcal{L}\mathcal{R})^2\,\mathcal{L}\mathcal{R}^2\,\mathcal{L}\mathcal{R}\,\mathcal{L}\mathcal{R}^2$	3
σ_7	$(\mathcal{R}\mathcal{L})^2\,\mathcal{R}\mathcal{L}^2\,\mathcal{R}\mathcal{L}\,\mathcal{R}\mathcal{L}^2$	3
σ_8	$\mathcal{R}\mathcal{L}\,\mathcal{R}\mathcal{L}^2\,\mathcal{R}\mathcal{L}\,(\mathcal{R}\mathcal{L}^2)^2$	3
σ_9	$\mathcal{R}\mathcal{L}^3\,(\mathcal{R}\mathcal{L}^2)^2$	2
σ_{10}	$\mathcal{R}\mathcal{L}^5$	1
σ_{11}	$\mathcal{L}\mathcal{R}\,\mathcal{L}\mathcal{R}^2\,\mathcal{L}\mathcal{R}\,(\mathcal{L}\mathcal{R}^2)^2\,\mathcal{L}\mathcal{R}\,\mathcal{L}\mathcal{R}^2\,(\mathcal{L}\mathcal{R}\,(\mathcal{L}\mathcal{R}^2)^2)^2$	4
σ_{12}	$\mathcal{L}\mathcal{R}\,(\mathcal{L}\mathcal{R}^2)^2\,\mathcal{L}\mathcal{R}\,\mathcal{L}\mathcal{R}^2\,\mathcal{L}\mathcal{R}\,(\mathcal{L}\mathcal{R}^2)^2\,(\mathcal{L}\mathcal{R}\,\mathcal{L}\mathcal{R}^2)^2$	4
σ_{13}	$\mathcal{L}\mathcal{R}^2\,(\mathcal{L}\mathcal{R})^2\,\mathcal{L}\mathcal{R}^2\,\mathcal{L}\mathcal{R}\,\mathcal{L}\mathcal{R}^2\,(\mathcal{L}\mathcal{R})^2\,(\mathcal{L}\mathcal{R}^2\,\mathcal{L}\mathcal{R})^2$	4
σ_{14}	$\mathcal{L}\mathcal{R}^2\,\mathcal{L}\mathcal{R}\,(\mathcal{L}\mathcal{R}^2\,(\mathcal{L}\mathcal{R})^2)^2\,\mathcal{L}\mathcal{R}^2\,\mathcal{L}\mathcal{R}\,\mathcal{L}\mathcal{R}^2\,(\mathcal{L}\mathcal{R})^2$	4
σ_{15}	$\mathcal{L}\mathcal{R}^2\,(\mathcal{L}\mathcal{R})^5$	2
σ_{16}	$\mathcal{R}\mathcal{L}\,(\mathcal{R}\mathcal{L}^2)^3\,(\mathcal{R}\mathcal{L}\,(\mathcal{R}\mathcal{L}^2)^2)^2$	3

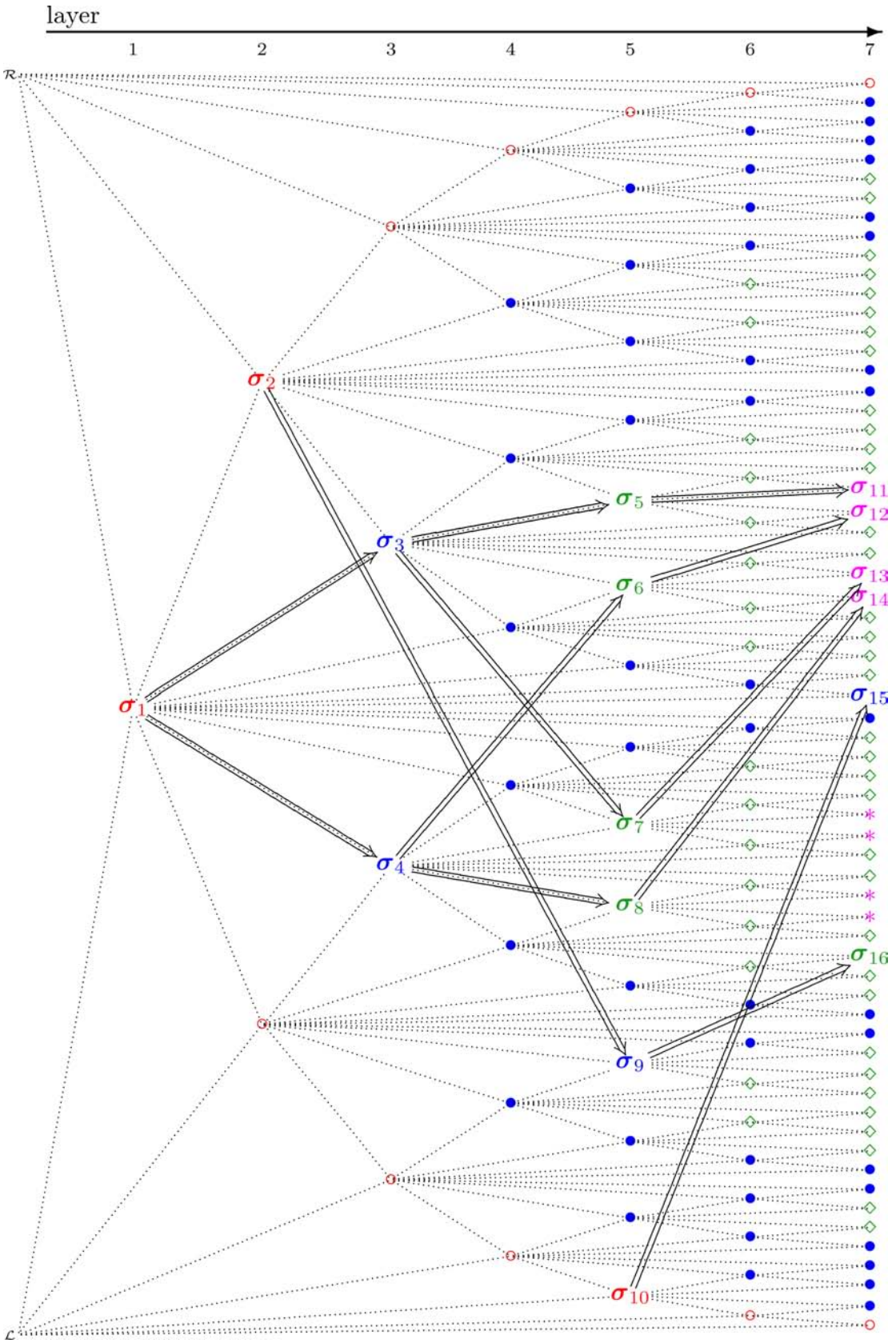

Fig. 7. Symbolic sequence adding scheme: preimages of some sequences. As in Fig. 6, the sequences of first, second, third and fourth complexity levels are shown as ○, ●, ◇, and ∗, respectively. The sequences labeled with σ_1 — σ_{16} are given in Table 1.

The question may arise why we start the paths from the sequences of the first complexity level and not from the one-symbol sequences $\mathcal{L}$ and $\mathcal{R}$. In fact, the complete symbolic sequence adding scheme can be created starting with these two symbols. As one can see, the family (58) results from the application of the replacement (64) to the one-symbol sequence $\mathcal{L}$ and the family (59) results from the application of the replacement (65) to the one-symbol sequence $\mathcal{R}$. However, this mode of operation is useful for the recursive creation of the symbolic sequences in the symbolic sequence adding scheme but not for the map replacement approach. The reason for this is given by the fact that for the recursive calculation of the border-collision bifurcation curves, as explained in Sec. 2, we need orbits which collide with the boundary in the state space from the left and from the right side. This is obviously not the case for the fixed points, since $O_{\mathcal{L}}$ collides with the boundary from the left side and $O_{\mathcal{R}}$ from the right side only.

3.3. *Colliding letters*

Let us note one further useful property of the described approach. As we have seen, to decide which replacement is admissible for the calculation of the bifurcation curves and which is not, we have to know the colliding letters in the starting sequence σ and in the target sequence ρ. In general, to find the two bifurcations (left and right), from the following three facts: (A) what are the colliding letters in σ, (B) what are the colliding letters in ρ, and (C) what are the admissible replacements leading from σ to ρ, only two are required and the third comes as a consequence. Typically, we use (A) and (B) to obtain (C). However, it is possible to use for example (A) and (C) to obtain (B). That means, if the colliding letters in the starting sequence σ are known and if it is also known that some replacement is admissible, then it becomes an easy task to determine the colliding letters in the target sequence ρ. As an example, let us consider the orbit O_ρ with

$$\rho = \mathcal{L}\mathcal{R}\mathcal{R}\mathcal{L}\mathcal{R}\mathcal{R}\mathcal{L}\mathcal{R}\mathcal{R}\mathcal{L}\mathcal{R}\mathcal{L}\mathcal{R}\mathcal{R}\mathcal{L}\mathcal{R}\mathcal{R}\mathcal{L}\mathcal{R}\mathcal{R}\mathcal{L}\mathcal{R}\mathcal{L}\mathcal{R}\mathcal{R}\mathcal{L}\mathcal{R}\mathcal{R}\mathcal{L}\mathcal{R}\mathcal{R}\mathcal{L}\mathcal{R}\mathcal{L}\mathcal{R}\mathcal{R}\mathcal{L}\mathcal{R}\mathcal{R}\mathcal{L}\mathcal{R} \tag{90}$$

It can be shown that the sequence ρ belongs to the symbolic sequence adding scheme. Calculating its preimages in this scheme we obtain

$$\begin{aligned} &\underline{\mathcal{L}}\mathcal{R}\mathcal{R}\underline{\mathcal{R}} \xrightarrow[]{\substack{\mathcal{L}\mapsto\mathcal{L}\mathcal{R}\mathcal{R}\\ \mathcal{R}\mapsto\mathcal{R}\mathcal{L}\mathcal{R}\mathcal{R}}} \underline{\mathcal{L}}\mathcal{R}\mathcal{R}\,\mathcal{R}\mathcal{L}\mathcal{R}\mathcal{R}\,\mathcal{R}\mathcal{L}\mathcal{R}\mathcal{R}\,\underline{\mathcal{R}}\mathcal{L}\mathcal{R}\mathcal{R} \\ &\xrightarrow[]{\substack{\mathcal{L}\mapsto\mathcal{L}\mathcal{R}\\ \mathcal{R}\mapsto\mathcal{R}\mathcal{L}\mathcal{R}}} \underline{\mathcal{L}}\mathcal{R}\,\mathcal{R}\mathcal{L}\mathcal{R}\mathcal{R}\mathcal{L}\mathcal{R}\mathcal{R}\mathcal{L}\mathcal{R}\,\mathcal{L}\mathcal{R}\,\mathcal{R}\mathcal{L}\mathcal{R}\mathcal{R}\mathcal{L}\mathcal{R}\mathcal{R}\mathcal{L}\mathcal{R}\,\mathcal{L}\mathcal{R}\,\mathcal{R}\mathcal{L}\mathcal{R}\mathcal{R}\mathcal{L}\mathcal{R}\underline{\mathcal{R}}\mathcal{L}\mathcal{R}\,\mathcal{L}\mathcal{R}\,\mathcal{R}\mathcal{L}\mathcal{R}\mathcal{R}\mathcal{L}\mathcal{R} \end{aligned} \tag{91}$$

and this leads us to conclude that the orbit O_ρ collides with the boundary with its first point from the left and with its 31st point from the right.

4. Period Adding: Border-Collision Bifurcations

Let us demonstrate the application of the map replacement approach in the case of the Σ/Δ-modulator model given by the map (3). This model is considered in several publications, where analytical expressions for the border-collision bifurcations involving periodic orbits of the family $\{O_{\mathcal{L}\mathcal{R}^n} \,|\, n > 0\}$ are used. Note that the sequences of these orbits correspond to the first generation of the symbolic sequences. Due to the symmetry of the map (3) given by

$$f(a, \mu, x) = -f(a, -\mu, -x) \tag{92}$$

the calculation of the border-collision bifurcations involving periodic orbits of the family $\{O_{\mathcal{R}\mathcal{L}^n} \,|\, n > 0\}$ is not necessary, as Eq. (92) implies that iff a periodic orbit $O_{\mathcal{L}\mathcal{R}^n}$ undergoes a border-collision bifurcation at parameter values (a^*, μ^*), then at the parameter values $(a^*, -\mu^*)$ the same bifurcation occurs for the periodic orbit $O_{\mathcal{R}\mathcal{L}^n}$. However, the bifurcation curves involving periodic orbits which are more complicated than $O_{\mathcal{L}\mathcal{R}^n}$ and $O_{\mathcal{R}\mathcal{L}^n}$ are typically calculated only numerically, because the analytical calculation becomes too complicated with increasing generation of the symbolic sequences. Now we are going to demonstrate that using the map replacement approach has become an easy task to calculate these curves analytically.

To simplify the notation we denote in the following periodic orbits corresponding to symbolic sequences of the ith complexity level as orbits of complexity level i. Similarly, the bifurcation curves for the orbits of complexity level i will be denoted as bifurcation curves of complexity level i.

4.1. *First complexity level*

According to the map replacement approach we start with the calculation of the bifurcation curves

for periodic orbits corresponding to symbolic sequences of the first complexity level, which are, as already mentioned in Sec. 3.1, the same as the sequences of the first generation of the general map (1). It is known that the existence region of the periodic orbit $O_{\mathcal{LR}^n}$ is bounded in the parameter space by border-collision bifurcation curves where the periodic orbit collides with the boundary $x = 0$ with its first point $x_0^{\mathcal{LR}^n}$ from the left side (corresponding to the letter $\mathcal{L}$) and with its last point $x_n^{\mathcal{LR}^n}$ from the right side (corresponding to the *last* letter $\mathcal{R}$). The same holds for periodic orbits $O_{\mathcal{RL}^n}$ up to an exchange of $\mathcal{L}$ with $\mathcal{R}$ and "left" with "right". Straight forward calculation shows that these points are given by

$$x_0^{\mathcal{LR}^n} = -\frac{-a_r^n\mu_l + a_r^n a_r\,\mu_\ell + \mu_r\,a_r^n - \mu_r}{-a_r^n a_\ell + a_r^{n+1}\,a_\ell + 1 - a_r} \tag{93}$$

$$x_n^{\mathcal{LR}^n} = -\frac{-a_r^{n-1}a_\ell\,\mu_r + a_r^n a_\ell\,\mu_r - a_r^{n-1}\mu_\ell + a_r^n\,\mu_\ell - \mu_r + \mu_r\,a_r^{n-1}}{-a_r^n a_\ell + a_r^{n+1}\,a_\ell + 1 - a_r} \tag{94}$$

$$x_0^{\mathcal{RL}^n} = -\frac{-a_\ell{}^n\mu_r + a_\ell^n a_\ell\,\mu_r + \mu_\ell\,a_\ell^n - \mu_\ell}{-a_\ell^n a_r + a_\ell^{n+1}a_r + 1 - a_\ell} \tag{95}$$

$$x_n^{\mathcal{RL}^n} = -\frac{-a_\ell^{n-1}a_r\,\mu_\ell + a_\ell^n a_r\,\mu_\ell - a_\ell^{n-1}\mu_r + a_\ell^n\,\mu_r - \mu_\ell + \mu_\ell\,a_\ell^{n-1}}{-a_\ell^n a_r + a_\ell^{n+1}a_r + 1 - a_\ell} \tag{96}$$

Then using the conditions $x_0^{\mathcal{LR}^n} = 0$ and $x_n^{\mathcal{LR}^n} = 0$, respectively, we obtain the border-collision bifurcation curves of the periodic orbits $O_{\mathcal{LR}^n}$ of first complexity level in the general map (1):

$$\xi_{\mathcal{LR}^n}^{\ell,0} = \left\{ (a_\ell, a_r, \mu_\ell, \mu_r) \;\middle|\; \frac{\mu_\ell}{\mu_r} = -\frac{a_r^n - 1}{a_r^n(a_r - 1)} \right\} \tag{97}$$

$$\xi_{\mathcal{LR}^n}^{r,n} = \left\{ (a_\ell, a_r, \mu_\ell, \mu_r) \;\middle|\; \frac{\mu_\ell}{\mu_r} = \frac{a_r^{n-1}(a_\ell - 1) - a_\ell a_r^n + 1}{a_r^{n-1}(a_r - 1)} \right\} \tag{98}$$

The bifurcation curves for the family $\{O_{\mathcal{RL}^n} \,|\, n > 0\}$ can be calculated either straight forward using the conditions $x_0^{\mathcal{RL}^n} = 0$ and $x_n^{\mathcal{RL}^n} = 0$, or more easily (due to the symmetry (2)) by exchanging the indexes ℓ and r in Eqs. (97) and (98). Either way we get

$$\xi_{\mathcal{RL}^n}^{r,0} = \left\{ (a_\ell, a_r, \mu_\ell, \mu_r) \;\middle|\; \frac{\mu_\ell}{\mu_r} = -\frac{a_\ell^n(a_\ell - 1)}{a_\ell^n - 1} \right\} \tag{99}$$

$$\xi_{\mathcal{RL}^n}^{\ell,n} = \left\{ (a_\ell, a_r, \mu_\ell, \mu_r) \;\middle|\; \frac{\mu_\ell}{\mu_r} = \frac{a_\ell^{n-1}(a_\ell - 1)}{a_\ell^{n-1}(a_r - 1) - a_\ell^n a_r + 1} \right\} \tag{100}$$

Comparing the bifurcation curves of the first complexity level calculated analytically [Fig. 8(b)] with the bifurcation structure calculated numerically [Fig. 8(a)], one can see quite a number of bifurcation curves which usually will not be calculated analytically (see for example Fig. 4.5 in [di Bernardo *et al.*, 2007]). In the next section we will show, that they can be easily calculated using the map replacement approach.

Note that the degenerated cases $a_{\ell/r} = 0$ and $a_{\ell/r} = 1$ are not considered here. Under this assumption the denominators in all expressions for bifurcation curves presented above are nonzero. In the degenerated cases the bifurcation curves can be calculated similarly but must be written in a different form.

4.2. *Second complexity level*

As a next step, let us calculate the border-collision bifurcation curves involving periodic orbits corresponding to sequences of the second complexity level. As stated above, there are four families of sequences in the second complexity level given by Eqs. (60)–(63). Recall that the bifurcation curves of the families given by Eqs. (60) and (63) result from the replacements (66) and (67), respectively, applied to

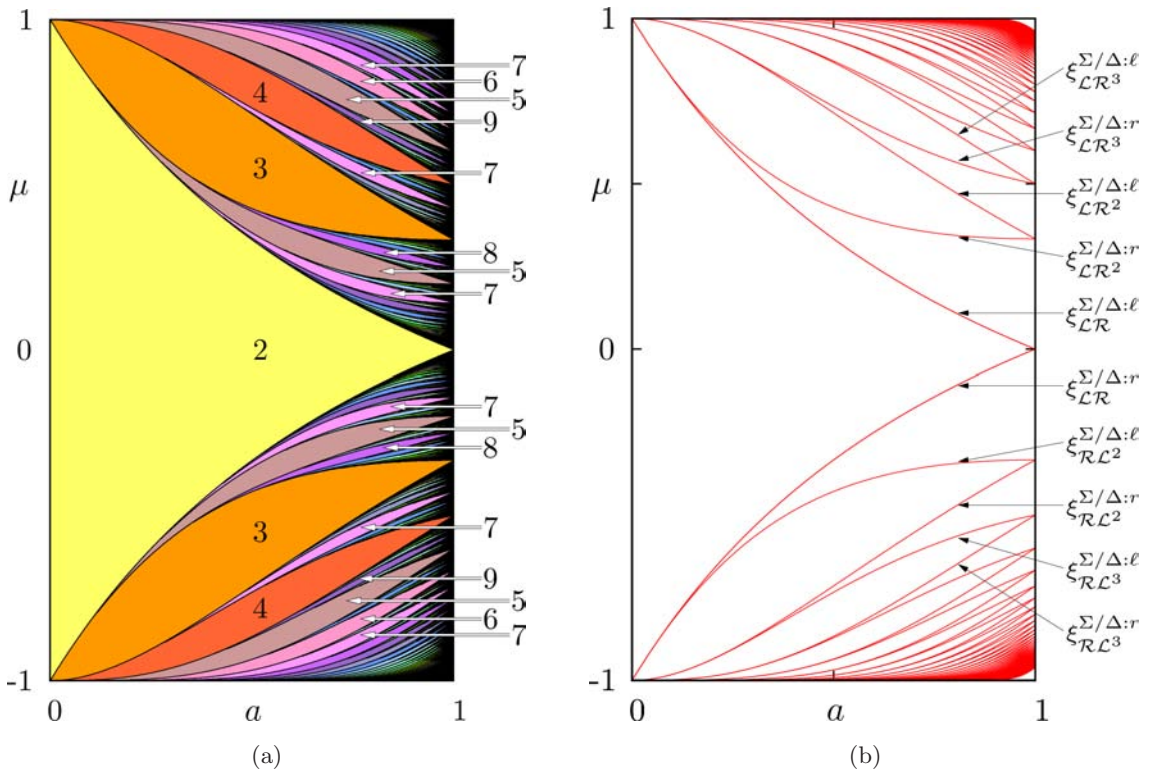

Fig. 8. (a) Numerically calculated bifurcation structure, with some of the periods marked. (b) Analytically calculated border-collision bifurcation curves $\xi^{\Sigma/\Delta:\ell,0}_{\mathcal{LR}^n}$, $\xi^{\Sigma/\Delta:r,0}_{\mathcal{RL}^n}$, $\xi^{\Sigma/\Delta:r,n}_{\mathcal{LR}^n}$ and $\xi^{\Sigma/\Delta:\ell,n}_{\mathcal{RL}^n}$ for $n = 1, \ldots, 50$.

the families (58) and (59). In other words, the bifurcation curves of the families (60) and (63) result from the application of the operators $\hat{\tau}^{\ell}_{n}$ and $\hat{\tau}^{r}_{n}$ on the families (58) and (59). Therefore, to calculate the bifurcation curves involving periodic orbits corresponding to the families given by Eqs. (60) and (61), we can use the following calculation schemes:

$$\begin{array}{ccc}
\xi^{\ell,0/r,n_1}_{\mathcal{LR}^{n_1}} & \xrightarrow[\substack{a_\ell \mapsto a_{\ell r^{n_2}} \quad a_r \mapsto a_{r\ell r^{n_2}} \\ \mu_\ell \mapsto \mu_{\ell r^{n_2}} \quad \mu_r \mapsto \mu_{r\ell r^{n_2}}}]{\hat{\tau}^{\ell}_{n_2}\begin{cases}\mathcal{L}\mapsto\mathcal{LR}^{n_2}\\ \mathcal{R}\mapsto\mathcal{RLR}^{n_2}\end{cases}} & \xi^{\ell,0/r,n_1(n_2+2)-1}_{\mathcal{LR}^{n_2}(\mathcal{RLR}^{n_2})^{n_1}} \\
 & & \Big\updownarrow \begin{cases}\mathcal{L}\mapsto\mathcal{R}\\ \mathcal{R}\mapsto\mathcal{L}\end{cases} \\
\xi^{\ell,n_1/r,0}_{\mathcal{RL}^{n_1}} & \xrightarrow[\substack{a_r \mapsto a_{r\ell^{n_2}} \quad a_\ell \mapsto a_{\ell r\ell^{n_2}} \\ \mu_r \mapsto \mu_{r\ell^{n_2}} \quad \mu_\ell \mapsto \mu_{\ell r\ell^{n_2}}}]{\hat{\tau}^{r}_{n_2}\begin{cases}\mathcal{L}\mapsto\mathcal{LRL}^{n_2}\\ \mathcal{R}\mapsto\mathcal{RL}^{n_2}\end{cases}} & \xi^{\ell,n_1(n_2+2)-1/r,0}_{\mathcal{RL}^{n_2}(\mathcal{LRL}^{n_2})^{n_1}}
\end{array} \tag{101}$$

The vertical double-arrow on the right side refers to the fact, that there are two equivalent possibilities to apply this scheme. The first one is to calculate the bifurcation curves $\xi^{\ell,0/r,n_1(n_2+2)-1}_{\mathcal{LR}^{n_2}(\mathcal{RLR}^{n_2})^{n_1}}$ from the curves $\xi^{\ell,0/r,n_1}_{\mathcal{LR}^{n_1}}$ by applying the operator $\hat{\tau}^{\ell}_{n_2}$ and after that to obtain the bifurcation curves $\xi^{r,n_1(n_2+2)-1/\ell,0}_{\mathcal{RL}^{n_2}(\mathcal{LRL}^{n_2})^{n_1}}$ from the bifurcation curves $\xi^{\ell,0/r,n_1(n_2+2)-1}_{\mathcal{LR}^{n_2}(\mathcal{RLR}^{n_2})^{n_1}}$ by exchanging the symbols $\mathcal{L}$ and $\mathcal{R}$ and the indexes ℓ and r. The second possibility is vice versa, that means the bifurcation curves $\xi^{r,n_1(n_2+2)-1/\ell,0}_{\mathcal{RL}^{n_2}(\mathcal{LRL}^{n_2})^{n_1}}$ can be calculated by applying the operator $\hat{\tau}^{r}_{n_2}$ to the bifurcation curves $\xi^{r,0/\ell,n_1}_{\mathcal{RL}^{n_1}}$. After that the bifurcation curves $\xi^{\ell,0/r,n_1(n_2+2)-1}_{\mathcal{LR}^{n_2}(\mathcal{LR}^{n_2+1})^{n_1}}$ will

be calculated from $\xi^{r,n_1(n_2+2)-1/\ell,0}_{\mathcal{RL}^{n_2}(\mathcal{RL}^{n_2+1})^{n_1}}$ by exchanging the symbols $\mathcal{L}$ and $\mathcal{R}$ and the indexes ℓ and r. The substitution coefficients $a_{\ell r^{n_2}/r\ell r^{n_2}}$, $a_{r\ell^{n_2}/\ell r\ell^{n_2}}$, $\mu_{\ell r^{n_2}/r\ell r^{n_2}}$ and $\mu_{r\ell^{n_2}/r\ell\ell^{n_2}}$ required by the calculation scheme (101) are defined by the coefficients of the functions f_ℓ and f_r iterated in the following way:

$$\begin{aligned} f_{\ell r^n}(x) &= f_r \circ \cdots \circ f_r \circ f_\ell(x) \\ &= \underbrace{a_\ell a_r^n}_{a_{\ell r^n}} x + \underbrace{\frac{-a_r^n\mu_\ell + a_r^{n+1}\mu_\ell + \mu_r\, a_r^n - \mu_r}{-1+a_r}}_{\mu_{\ell r^n}} \end{aligned} \tag{102}$$

$$\begin{aligned} f_{r\ell r^n}(x) &= f_r \circ \cdots \circ f_r \circ f_\ell \circ f_r(x) \\ &= \underbrace{a_\ell a_r^{n+1}}_{a_{r\ell r^n}} x + \underbrace{\frac{-a_r^n a_\ell\,\mu_r + a_r^{n+1} a_\ell\,\mu_r - a_r^n\mu_\ell + a_r^{n+1}\mu_\ell - \mu_r + \mu_r\, a_r^n}{-1+a_r}}_{\mu_{r\ell r^n}} \end{aligned} \tag{103}$$

$$\begin{aligned} f_{r\ell^n}(x) &= f_\ell \circ \cdots \circ f_\ell \circ f_r(x) \\ &= \underbrace{a_\ell^n a_r}_{a_{r\ell^n}} x + \underbrace{\frac{-a_\ell^n\mu_r + a_\ell^{n+1}\mu_r + \mu_\ell\, a_\ell^n - \mu_\ell}{-1+a_\ell}}_{\mu_{r\ell^n}} \end{aligned} \tag{104}$$

$$\begin{aligned} f_{\ell r\ell^n}(x) &= f_\ell \circ \cdots \circ f_\ell \circ f_r \circ f_\ell(x) \\ &= \underbrace{a_\ell^{n+1} a_r}_{a_{\ell r\ell^n}} x + \underbrace{\frac{-a_\ell^n a_r\,\mu_\ell + a_\ell^{n+1} a_r\,\mu_\ell - a_\ell^n\mu_r + a_\ell^{n+1}\mu_r - \mu_\ell + \mu_\ell\, a_\ell^n}{-1+a_\ell}}_{\mu_{\ell r\ell^n}} \end{aligned} \tag{105}$$

Note that the general parameter n in Eqs. (102)–(105) has to be replaced by the particular value given by the used specific operator, which was n_2 in the example above.

Similarly, the families given by Eqs. (62) and (63) result from the application of the operators $\hat\tau_n^\ell$ and $\hat\tau_n^r$ on the families (58) and (59). Therefore, the calculation schemes are given in this case by

$$\begin{array}{ccc} \xi^{\ell,0/r,n_1}_{\mathcal{LR}^{n_1}} & \xrightarrow[\substack{a_r \mapsto a_{r\ell^{n_2}} \quad a_\ell \mapsto a_{\ell r\ell^{n_2}} \\ \mu_r \mapsto \mu_{r\ell^{n_2}} \quad \mu_\ell \mapsto \mu_{\ell r\ell^{n_2}}}]{\hat\tau_{n_2}^r \begin{cases} \mathcal{L} \mapsto \mathcal{LRL}^{n_2} \\ \mathcal{R} \mapsto \mathcal{RL}^{n_2} \end{cases}} & \xi^{\ell,0/r,n_1(n_2+1)+1}_{\mathcal{LRL}^{n_2}(\mathcal{RL}^{n_2})^{n_1}} \\ & & \Big\updownarrow \begin{cases} \mathcal{L} \mapsto \mathcal{R} \\ \mathcal{R} \mapsto \mathcal{L} \end{cases} \\ \xi^{\ell,n_1/r,0}_{\mathcal{RL}^{n_1}} & \xrightarrow[\substack{a_\ell \mapsto a_{\ell r^{n_2}} \quad a_r \mapsto a_{r\ell r^{n_2}} \\ \mu_\ell \mapsto \mu_{\ell r^{n_2}} \quad \mu_r \mapsto \mu_{r\ell r^{n_2}}}]{\hat\tau_{n_2}^\ell \begin{cases} \mathcal{L} \mapsto \mathcal{LR}^{n_2} \\ \mathcal{R} \mapsto \mathcal{RLR}^{n_2} \end{cases}} & \xi^{\ell,n_1(n_2+1)+1/r,0}_{\mathcal{RLR}^{n_2}(\mathcal{LR}^{n_2})^{n_1}} \end{array} \tag{106}$$

Again, due to the symmetry (2), there are two equivalent calculation ways, one of them using the operator $\hat\tau_{n_2}^\ell$ and the other using the operator $\hat\tau_{n_2}^r$. Consequently, all four families of bifurcation curves of the second complexity level can be calculated using only one operator (either $\hat\tau_{n_2}^\ell$ or $\hat\tau_{n_2}^r$). Hence, from the eight replacement coefficients defined by Eqs. (102)–(105) only four are really needed for the calculation.

Let us demonstrate the described procedure using the families of periodic orbits corresponding to the sequences given by Eqs. (60) and (61). According to the calculation scheme (101) we

substitute the coefficients $a_{\ell r^n/r\ell r^n}$ and $\mu_{\ell r^n/r\ell r^n}$ into Eqs. (97)–(100) and obtain the expressions for these bifurcation curves:

$$\xi^{\ell,0}_{\mathcal{LR}^{n_2}(\mathcal{RLR}^{n_2})^{n_1}} = \left\{ (a_\ell, a_r, \mu_\ell, \mu_r) \;\middle|\; \frac{\mu_{\ell r^{n_2}}}{\mu_{r\ell r^{n_2}}} = -\frac{a^{n_2}_{r\ell r^{n_2}} - 1}{a^{n_2}_{r\ell r^{n_2}}\,(a_{r\ell r^{n_2}} - 1)} \right\} \tag{107}$$

$$\xi^{r,n_1(n_2+2)}_{\mathcal{LR}^{n_2}(\mathcal{RLR}^{n_2})^{n_1}} = \left\{ (a_\ell, a_r, \mu_\ell, \mu_r) \;\middle|\; \frac{\mu_{\ell r^{n_2}}}{\mu_{r\ell r^{n_2}}} = \frac{a_{\ell r^{n_2}} - a_{r\ell r^{n_2}}\, a_{\ell r^{n_2}} + a^{-n_2+1}_{r\ell r^{n_2}} - 1}{-1 + a_{r\ell r^{n_2}}} \right\} \tag{108}$$

$$\xi^{r,0}_{\mathcal{LR}^{n_2+1}(\mathcal{LR}^{n_2})^{n_1}} = \left\{ (a_\ell, a_r, \mu_\ell, \mu_r) \;\middle|\; \frac{\mu_{\ell r^{n_2}}}{\mu_{r\ell r^{n_2}}} = -\frac{a^{n_2}_{\ell r^{n_2}}\,(a_{\ell r^{n_2}} - 1)}{-1 + a^{n_2}_{\ell r^{n_2}}} \right\} \tag{109}$$

$$\xi^{\ell,n_1(n_2+1)+2}_{\mathcal{RLR}^{n_2}(\mathcal{LR}^{n_2})^{n_1}} = \left\{ (a_\ell, a_r, \mu_\ell, \mu_r) \;\middle|\; \frac{\mu_{\ell r^{n_2}}}{\mu_{r\ell r^{n_2}}} = \frac{a^{n_2}_{\ell r^{n_2}}\,(a_{\ell r^{n_2}} - 1)}{a^{n_2}_{\ell r^{n_2}} a_{r\ell r^{n_2}} - a^{n_2+1}_{\ell r^{n_2}} a_{r\ell r^{n_2}} + a_{\ell r^{n_2}} - a^{n_2}_{\ell r^{n_2}}} \right\} \tag{110}$$

Equations (107)–(110) can be easily resolved with respect to the original parameters $a_{\ell/r}$, $\mu_{\ell/r}$. This leads us to the final result for the bifurcations involving the orbits $O_{\mathcal{LR}^{n_2}(\mathcal{LR}^{n_2+1})^{n_1}}$

$$\xi^{\ell,0}_{\mathcal{LR}^{n_2}(\mathcal{RLR}^{n_2})^{n_1}} = \left\{ (a_\ell, a_r, \mu_\ell, \mu_r) \;\middle|\; \frac{\mu_\ell}{\mu_r} = \frac{N}{D} \right\} \tag{111}$$

$$N = a_\ell^{n_1+1} a_r^{n_1 n_2 + n_1 + 2n_2 + 1} - a_\ell^{n_1+1} a_r^{n_1 n_2 + n_1 + n_2} + a_\ell a_r^{n_2} - a_\ell a_r^{n_2+1} + 1 - a_r^{n_2}$$

$$D = a_\ell^{n_1+1} a_r^{n_1 n_2 + n_1 + 2n_2 + 1} - a_\ell^{n_1+1} a_r^{n_1 n_2 + n_1 + 2n_2 + 2} - a_r^{n_2} + a_r^{n_2+1}$$

$$\xi^{r,n_1(n_2+2)}_{\mathcal{LR}^{n_2}(\mathcal{RLR}^{n_2+1})^{n_1}} = \left\{ (a_\ell, a_r, \mu_\ell, \mu_r) \;\middle|\; \frac{\mu_\ell}{\mu_r} = \frac{N}{D} \right\} \tag{112}$$

$$\begin{aligned} N = {} & a_\ell^{-n_1+1} a_r^{n_1 n_2 - n_1 + 2n_2 + 1} - a_\ell^3 a_r^{3n_2+2} + 2a_\ell^2 a_r^{2n_2+1} + a_\ell^3 a_r^{3n_2+1} \\ & - a_\ell\, a_r^{2n_2+1} + a_\ell^{2-n_1} a_r^{-n_1 n_2 - n_1 + 2n_2 + 1} - a_\ell^{2-n_1}\, a_r^{n_1 n_2 - n_1 + 2n_2 + 1} \\ & - a_\ell^2 a_r^{3n_2+1} - a_\ell^2 a_r^{2n_2} - a_\ell a_r^{2n_2} - a_\ell^{-n_1+1} a_r^{-n_1 n_2 - n_1 + n_2 + 1} \end{aligned}$$

$$\begin{aligned} D = {} & -a_\ell^{-n_1+1} a_r^{-n_1 n_2 - n_1 + 2n_2 + 2} + a_\ell^{-n_1+1} a_r^{-n_1 n_2 - n_1 + 2n_2 + 1} - 2a_\ell a_r^{2n_2+1} \\ & + a_\ell a_r^{2n_2+1} + a_\ell a_r^{2n_2} + a_\ell^2 a_r^{3n_2+2} - a_\ell^2 a_r^{3n_2+1} \end{aligned}$$

and for the bifurcations involving the orbits $O_{(\mathcal{LR}^{n_2+1})(\mathcal{LR}^{n_2})^{n_1}}$

$$\xi^{\ell,n_1(n_2+1)+2}_{\mathcal{RLR}^{n_2}(\mathcal{LR}^{n_2})^{n_1}} = \left\{ (a_\ell, a_r, \mu_\ell, \mu_r) \;\middle|\; \frac{\mu_\ell}{\mu_r} = \frac{N}{D} \right\} \tag{113}$$

$$N = a_\ell^{n_1 n_2 + n_1 + 2n_2 + 1}\, a_r^{n_1+1} - a_\ell^{(n_1+2)(n_2+1)}\, a_r^{n_1+1} - a_\ell^{n_2} - a_\ell^{n_2+1}$$

$$D = a_\ell^{n_1 n_2 + n_1 + 2n_2 + 1}\, a_r^{n_1+1} - a_\ell^{n_1 n_2 + n_1 + n_2}\, a_r^{n_1+1} + a_\ell^{n_2} a_r - a_\ell^{n_2+1} a_r + 1 - a_\ell^{n_2}$$

$$\xi^{r,0}_{\mathcal{RLR}^{n_2}(\mathcal{LR}^{n_2})^{n_1}} = \left\{ (a_\ell, a_r, \mu_\ell, \mu_r) \;\middle|\; \frac{\mu_\ell}{\mu_r} = \frac{N}{D} \right\} \tag{114}$$

$$\begin{aligned} N = {} & -a_\ell^{n_1 n_2 + n_1 + n_2} a_r^{n_1} - a_\ell^{n_2+2+n_1 n_2 + n_1} a_r^{n_1} + 2a_\ell^{(n_1+1)(n_2+1)} a_r^{n_1} \\ & a_\ell^{n_1 n_2 + n_1 + 2n_2 + 1} a_r^{n_1+1} - a_\ell^{(n_1+2)(n_2+1)} a_r^{n_1+1} + a_\ell^{n_2+2} - a_\ell^{n_2+1} \end{aligned}$$

$$\begin{aligned} D = {} & -a_\ell^{n_1 n_2 + n_1 + 2n_2 + 1} a_r^{n_1+2} - 2a_\ell^{(n_1+1)(n_2+1)} a_r^{n_1+1} + a_\ell^{(n_1+2)(n_2+1)} a_r^{n_1+2} \\ & + a_\ell^{n_1 n_2 + n_1 + 2n_2 + 1} a_r^{n_1+1} + a_\ell^{n_2+1} a_r - a_\ell^{n_2+2} a_r + a_\ell^{(n_1+1)(n_2+1)} a_r^{n_1} + a_\ell \\ & + a_\ell^{n_1 n_2 + n_1 + n_2} a_r^{n_1+1} - a_\ell^{n_2+1} - a_\ell^{n_1 n_2 + n_1 + n_2} a_r^{n_1} \end{aligned}$$

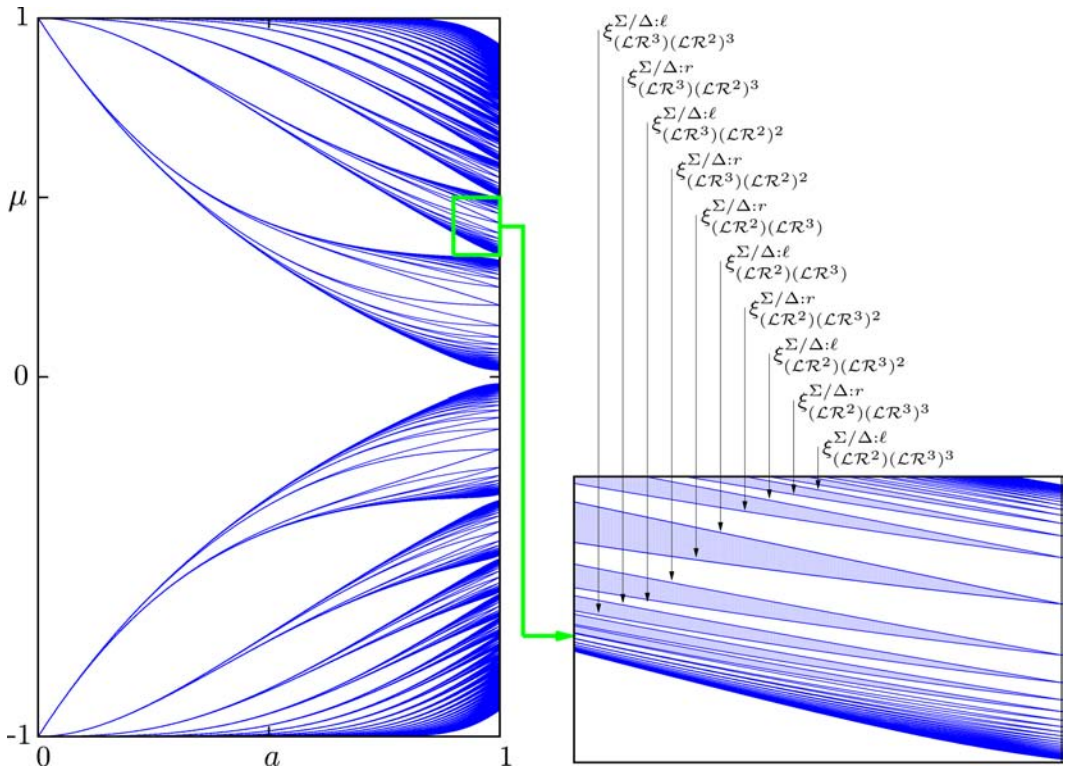

Fig. 9. Analytically calculated border-collision bifurcation curves of second complexity level for $n_1 = 1, \ldots, 25$, $n_2 = 1, \ldots, 25$. The marked rectangle in the left figure is shown enlarged in the right figure where some of the bifurcation curves are labeled.

As already stated, the remaining four bifurcation curves can be obtained by exchanging the indexes ℓ and r in Eqs. (111)–(114).

For the visualization of the results we use again the map (3). The substitution (4) leads us to the bifurcation curves of the second complexity level for this map, shown in Fig. 9. Note that this figure shows 1250 bifurcation curves calculated analytically and reflects the bifurcation structure calculated numerically almost completely. Adding the bifurcation curves of the third complexity level we will obtain a structure which is really difficult to distinguish from the numerical results.

4.3. *Third complexity level*

As a next step, we wish to calculate the bifurcation curves for the orbits of the third complexity level. Recall that there are eight three-parametric families of the symbolic sequences in this level [see Eqs. (69)–(76)], so we have to calculate eight pairs of families of bifurcation curves. By contrast to the second complexity level, where the calculation scheme is unique for each family, in the third complexity level there are two possible ways for calculation.

Let us consider, for example, the family of orbits corresponding to the sequences of the third complexity level given by Eq. (69). It can be easily seen that this family can be obtained from the family (58) of the first complexity level using the following two-parametric replacement:

$$\hat{\tau}^{\ell}_{n_3} \circ \hat{\tau}^{\ell}_{n_2} := \begin{cases} \mathcal{L} \mapsto \mathcal{LR}^{n_3} (\mathcal{RLR}^{n_3})^{n_2} \\ \mathcal{R} \mapsto \mathcal{RLR}^{n_3} \mathcal{LR}^{n_3} (\mathcal{RLR}^{n_3})^{n_2} \end{cases} \tag{115}$$

which represents a consecutive application of the operators $\hat{\tau}^{\ell}_{n_3}$ and $\hat{\tau}^{\ell}_{n_2}$. The same replacement leads from the family (59) to the family given by Eq. (70). The remaining six families of sequences [Eqs. (71)–(76)] of the third complexity level can be calculated from the corresponding sequences of the first complexity level using similar composite operators $\hat{\tau}^{r}_{n_3} \circ \hat{\tau}^{\ell}_{n_2}$, $\hat{\tau}^{\ell}_{n_3} \circ \hat{\tau}^{r}_{n_2}$ and $\hat{\tau}^{r}_{n_3} \circ \hat{\tau}^{r}_{n_2}$. This calculation scheme is illustrated in Fig. 10(a). Hence, to calculate the bifurcation curves for orbits of the third complexity level, one has to calculate four sets of four substitution coefficients each, defined analogously to the two sets of four substitution coefficients given by Eqs. (102)–(105). After that, one has to substitute the coefficients into Eqs. (97) and (98). Of course, half of the calculations can be avoided if

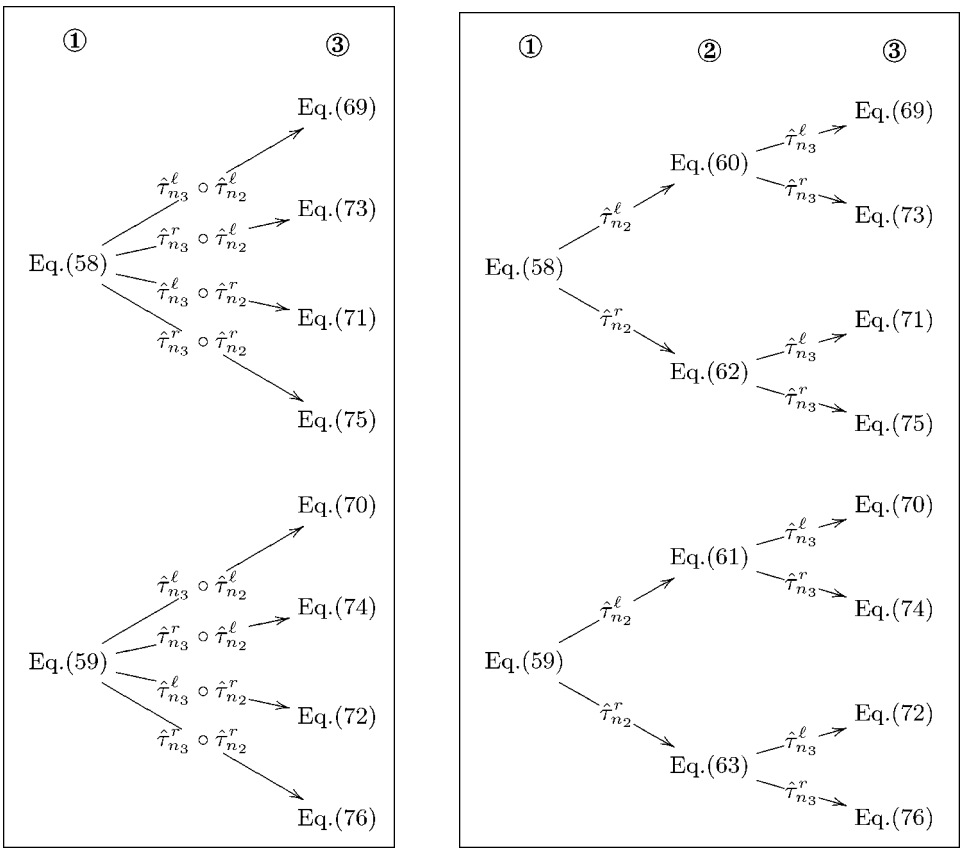

(a) (b)

Fig. 10. Nonrecursive (a) versus recursive (b) calculation of the bifurcation curves for the families of complexity level 3. Specific families of symbolic sequences are labeled with their corresponding equation numbers. Circled numbers refer to complexity levels. In the nonrecursive case the calculation is done in one step starting with the families of complexity level 1 and requires four new (composite) replacement operators. By contrast, the recursive calculation for the families of complexity level 3 uses the same two operators as already used for the calculation of the families of complexity level 2.

the considered map has a symmetry similar to the one given by Eq. (2), as it was demonstrated for the map (1) and the bifurcation curves of the second complexity level. Nevertheless, the described calculation scheme is not the most efficient one.

To demonstrate a more efficient calculation scheme, let us note that the described procedure represents a *nonrecursive* application of the map replacement approach. That means, the bifurcation curves of the third, fourth and all further complexity levels can be calculated using the bifurcation curves of the first complexity level. However, this requires a recalculation of the substitution coefficients in each step. Recall that there are 2^i families of sequences in the complexity level i. To calculate the bifurcation curves of the orbits corresponding to all these families, 2^{i-1} sets of substitution coefficients are required. For systems with a symmetry similar to Eq. (2) only 2^{i-2} sets of substitution coefficients are required. Therefore, when calculating the bifurcation curves for all orbits up to a certain complexity level, it is more efficient to use explicitly the recursive definition of the symbolic sequence adding scheme. Recall that all $8 = 2^3$ families of sequences of the third complexity level can be obtained from the $4 = 2^2$ families of the second complexity level using the operators $\hat{\tau}^{\ell}_{n_3}$ and $\hat{\tau}^{r}_{n_3}$. Hence, we can replace the coefficients in the equations of the bifurcation curves for the 2^2 families of orbits of the second complexity level by the already calculated substitution coefficients (102)–(105) and obtain the bifurcation curves for the 2^3 families of orbits of the third complexity level. This recursive calculation scheme is illustrated in Fig. 10(b). Of course, the symmetry of the map (1) leads to the possibility to calculate the bifurcation curves for only four of these families and to obtain the bifurcation curves for the remaining four families by exchanging the indexes ℓ and r. As an example, for the bifurcation curves involving

the orbits corresponding to the sequences given by Eqs. (69) and (76) we get the following calculation schemes:

$$\xi^{\ell,0/r,n_1(n_2+2)-1}_{\mathcal{LR}^{n_2}(\mathcal{RLR}^{n_2})^{n_1}} \xrightarrow[\substack{a_\ell \mapsto a_{\ell r^{n_3}} \quad a_r \mapsto a_{r\ell r^{n_3}} \\ \mu_\ell \mapsto \mu_{\ell r^{n_3}} \quad \mu_r \mapsto \mu_{r\ell r^{n_3}}}]{\hat{\tau}^{\ell}_{n_3}\begin{cases}\mathcal{L}\mapsto\mathcal{LR}^{n_3}\\ \mathcal{R}\mapsto\mathcal{RLR}^{n_3}\end{cases}} \xi^{\ell,0/r,\ {}^{n_1(n_2+1)(n_3+2)+}_{(n_1-1)(n_3+1)-1}}_{\substack{\mathcal{LR}^{n_3}(\mathcal{RLR}^{n_3})^{n_2}\\ (\mathcal{RLR}^{n_3}\mathcal{LR}^{n_3}(\mathcal{RLR}^{n_3})^{n_2})^{n_1}}}$$

$$\Big\downarrow \begin{cases}\mathcal{L}\mapsto\mathcal{R}\\ \mathcal{R}\mapsto\mathcal{L}\end{cases} \tag{116}$$

$$\xi^{\ell,n_1(n_2+2)-1/r,0}_{\mathcal{RL}^{n_2}(\mathcal{RLL}^{n_2})^{n_1}} \xrightarrow[\substack{a_r \mapsto a_{r\ell^{n_3}} \quad a_\ell \mapsto a_{\ell r\ell^{n_3}} \\ \mu_r \mapsto \mu_{r\ell^{n_3}} \quad \mu_\ell \mapsto \mu_{\ell r\ell^{n_3}}}]{\hat{\tau}^{r}_{n_3}\begin{cases}\mathcal{L}\mapsto\mathcal{RL}^{n_3}\\ \mathcal{R}\mapsto\mathcal{RL}^{n_3}\end{cases}} \xi^{\ell,\ {}^{n_1(n_2+1)(n_3+2)+}_{(n_1-1)(n_3+2)-1}/r,0}_{\substack{\mathcal{RL}^{n_3}(\mathcal{LRL}^{n_3})^{n_2}\\ (\mathcal{LRL}^{n_3}\mathcal{RL}^{n_3}(\mathcal{LRL}^{n_3})^{n_2})^{n_1}}}$$

Similar calculation schemes allow us the calculation of all bifurcation curves for the orbits corresponding to the remaining sequences of the third complexity level. The resulting expressions are too long for being presented here (for example, the numerator in the bifurcation curve $\xi^{\ell,0}_{\mathcal{LR}^{n_3}(\mathcal{LR}^{n_3+1})^{n_2}(\mathcal{LR}^{n_3}(\mathcal{LR}^{n_3+1})^{n_2+1})^{n_1}}$ contains 17 terms) but can be easily obtained using computer algebra software like Maple or Mathematica. The obtained bifurcation curves for all eight families of orbits of the third complexity level for the map (3) are shown in Fig. 11.

The calculation of the bifurcation curves for further complexity levels can be performed in the same way. For example, for the recursive calculation of the bifurcation curves of the fourth complexity level we can use the curves of the third complexity level and the same substitution coefficients (102)–(105). In general there are 2^{i-2} possible ways to

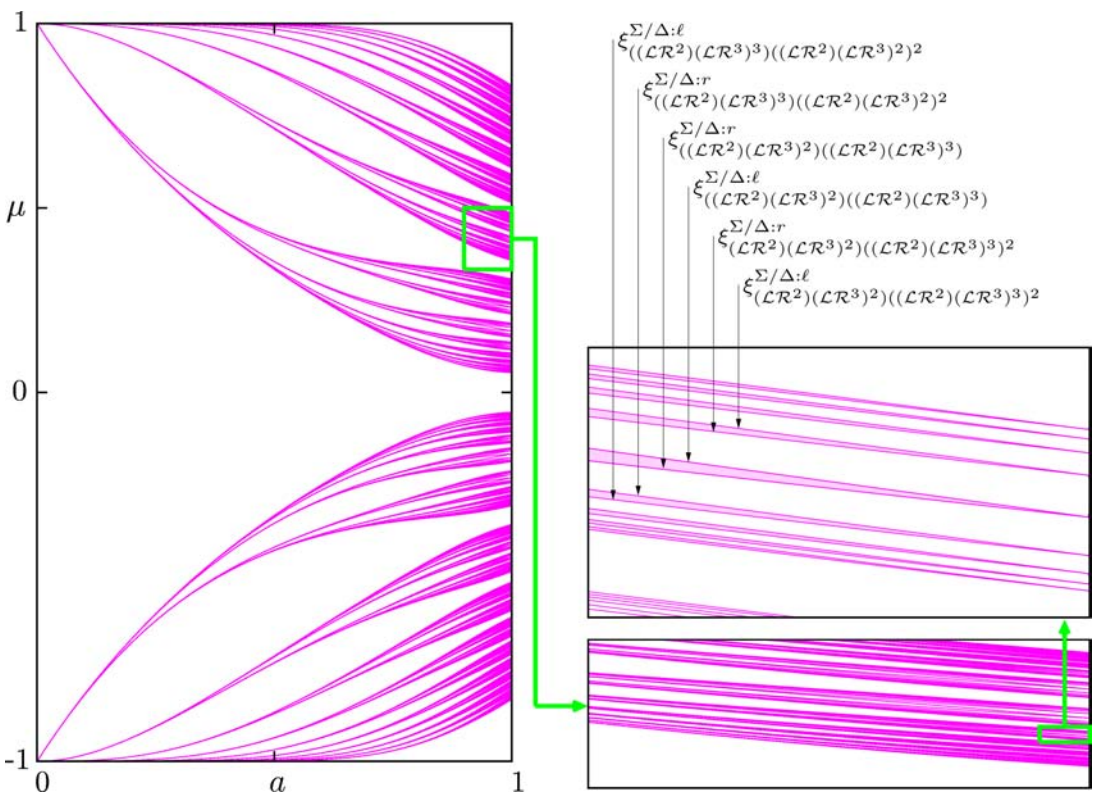

Fig. 11. Border-collision bifurcation curves of third complexity level calculated analytically for $n_1 = 1, \ldots, 25$, $n_2 = 1, \ldots, 10$, $n_3 = 1, \ldots, 5$. The marked rectangles are shown enlarged, some of the bifurcation curves are labeled.

calculate the bifurcation curves of a given family of complexity level i. One of them uses only the operators $\hat{\tau}^{\ell}_{n_i}$ and $\hat{\tau}^{r}_{n_i}$ whereas all other calculation ways require composite operators. This is obvious, because the number of possible calculation ways $W(i)$ for complexity level i is determined by the sum over the possible ways of calculation of all lower complexity levels, that means: $W(i) = \sum_{k=1}^{i-1} W(k)$ with $W(1) = 1$. As an example, one can see that the same family of the fourth complexity levels can be calculated either by applying the composite operator $\hat{\tau}^{\ell}_{n_4} \circ \hat{\tau}^{\ell}_{n_3} \circ \hat{\tau}^{\ell}_{n_2}$ to the family of the first complexity level given by Eq. (58) or by applying the composite operator $\hat{\tau}^{\ell}_{n_4} \circ \hat{\tau}^{\ell}_{n_3}$ to the family of the second complexity level given by Eq. (60) or by applying the operator $\hat{\tau}^{\ell}_{n_4}$ to the family of the third complexity level given by Eq. (69) for which we have already two ways of calculation. Of course, the resulting expressions for the bifurcation curves are quite long (the number of terms in the numerators of the bifurcation curves of the fourth complexity level is between 29 and 53), but can be calculated straight forward.

5. Embedding of the Bifurcation Curves and Self-Similarity

Finally let us provide a geometrical interpretation of the presented results concerning the period-adding structure. This can be done more easily considering the results obtained for the 2D parameter space of map (3), although the same interpretation is valid for the 2D parameter space of the general map (1). Recall that in each calculation step we used the operators $\hat{\tau}^{\ell}_{n}$ and $\hat{\tau}^{r}_{n}$ defined in the space of admissible symbolic sequences.

With each of these operators a mapping $\mathbb{R}^2 \to \mathbb{R}^2$ in the 2D parameter space $a \times \mu$ of map (3), denoted in the following by $\hat{\phi}^{\ell}_{n}$ and $\hat{\phi}^{r}_{n}$, respectively, can be associated. This mapping defines a correspondence between the region in the parameter space where some bifurcation curve ζ_σ is located, and the region containing the bifurcation curves $\zeta_{\hat{\tau}^{\ell}_{n}(\sigma)}$ and $\zeta_{\hat{\tau}^{r}_{n}(\sigma)}$, respectively.

Let us denote the rectangular region $a \in [0, 1]$, $\mu \in [-1, 1]$ containing the period-adding structure by R and its corner points by A, B, C and D as shown in Fig. 12. Then $\hat{\phi}^{\ell}_{1}$ maps R onto the

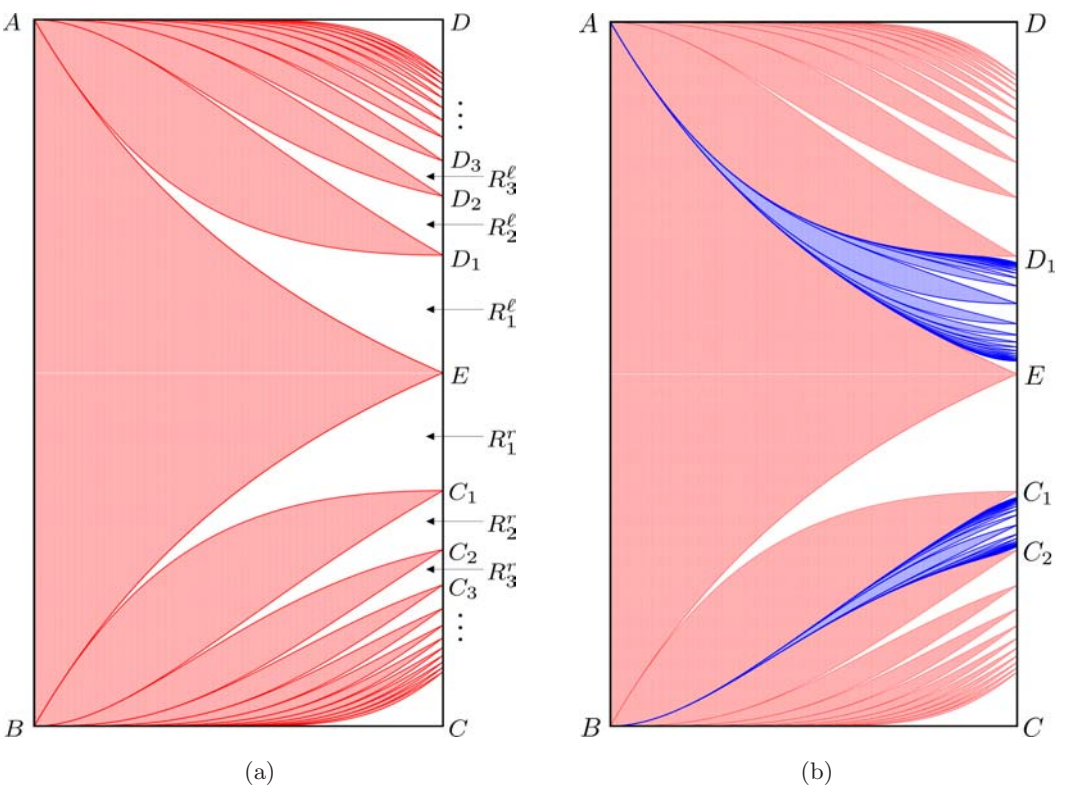

Fig. 12. (a) Region R (rectangle $ABCD$) and its images $R_i^{\ell/r}$ (shown white) under the application of the mappings $\hat{\phi}_i^{\ell/r}$ for $i = 1, 2, 3$. (b) Regions bounded by the bifurcation curves of the first complexity level (shown red in both figures) and the images of these regions (shown blue) by the mappings $\hat{\phi}^{\ell}_{1}$ and $\hat{\phi}^{r}_{2}$ (bounded by the bifurcation curves of the second complexity level located in R^{ℓ}_{1} and R^{r}_{2}, respectively).

triangular-like region R_1^ℓ as follows: the complete segment AB is mapped onto the point A, the segment CD is mapped onto the segment ED_1, the segment AD is mapped onto the curve $AD_1 \equiv \xi_{\mathcal{LR}^2}^{\Sigma/\Delta:r}$, and the segment BC is mapped onto the curve $AE \equiv \xi_{\mathcal{LR}}^{\Sigma/\Delta:\ell}$. Similarly, $\hat{\phi}_1^r$ maps R onto the region R_1^r: the segment AB is mapped onto the point B, the segment CD is mapped onto the segment C_1E, the segment AD is mapped onto the curve $BE \equiv \xi_{\mathcal{LR}}^{\Sigma/\Delta:r}$, and the segment BC is mapped onto the curve $BC_1 \equiv \xi_{\mathcal{RL}^2}^{\Sigma/\Delta:\ell}$. Figure 12(a) shows the images $R_i^{\ell/r}$ of the region R under the application of the mappings $\hat{\phi}_i^{\ell/r}$ for $i = 1, 2, 3$. As one can see, these images (shown white) are located between the periodicity regions of the orbits of the first level of complexity (shown red). Hereby, all bifurcation curves of the first complexity level contained in R are mapped by $\hat{\phi}_1^\ell$ (respectively, $\hat{\phi}_1^r$) onto the bifurcation curves of the second complexity level contained in R_1^ℓ (respectively, R_1^r). For example, Fig. 12(b) shows the images of the periodicity regions of the orbits of the first level of complexity by the mappings $\hat{\phi}_1^\ell$ and $\hat{\phi}_2^r$. Of course, this mapping process can be continued *ad infinitum*. In other words: applying the transformation $\hat{\phi}_1^\ell$ to *all* the bifurcation curves of the first complexity level in R, we obtain *all* the bifurcation curves of the second complexity level inside R_1^ℓ, and similarly, applying the transformation $\hat{\phi}_n^\ell$ to all the bifurcation curves of the first complexity level in R we obtain all the bifurcation curves of the second complexity level inside R_n^ℓ. In the same way, the transformation $\hat{\phi}_n^r$ maps all bifurcation curves of the first complexity level in R on all bifurcation curves of the second complexity level inside R_n^r.

6. Conclusions and Outlook

We presented in this work, the map replacement approach, which allows us to calculate bifurcation curves in a very efficient and elegant way. Our work follows and extends the brilliant work by Leonov, which was published already in 1959 but remained unfortunately mainly unregarded. Although we demonstrated the approach by considering border-collision bifurcations, it is also applicable to other types of bifurcations like for example crisis bifurcations in the chaotic domain. The class of dynamical systems for which the approach is applicable includes not only 1D piecewise-linear maps but also multidimensional piecewise-linear maps as well as piecewise-linear-fractional maps. As these systems appear naturally in many applications and are therefore intensively investigated, the map replacement approach might accelerate this research.

References

Avrutin, V., Schanz, M. & Banerjee, S. [2006] "Multiparametric bifurcations in a piecewise-linear discontinuous map," *Nonlinearity* **19**, 1875–1906.

Avrutin, V. & Schanz, M. [2008] "On the fully developed bandcount adding scenario," *Nonlinearity* **21**, 1077–1103.

Avrutin, V. & Schanz, M. [2009] "Self-similarity of the bandcount adding: Calculation by map replacement," *Proc. Int. Workshop on Nonlinear Maps and their Applications* (*NOMA'09*), Urbino, Italy, pp. 62–66.

Bai-Lin, H. [1989] *Elementary Symbolic Dynamics and Chaos in Dissipative Systems* (World Scientific, Singapore).

Brocot, A. [1861] "Calcul des rouages par approximation, nouvelle méthode," *Revue Chronometrique* **3**, 186–194.

Coutinho, R., Fernandez, B., Lima, R. & Meyroneine, A. [2006] "Discrete time piecewise affine models of genetic regulatory networks," *J. Math. Biol.* **52**, 524–570.

di Bernardo, M., Budd, C. J., Champneys, A. R. & Kowalczyk, P. [2007] *Piecewise-Smooth Dynamical Systems: Theory and Applications*, Applied Mathematical Sciences, Vol. 163 (Springer).

Farey, J. [1816] "On a curious property of vulgar fractions," *Philos. Mag. J.* **47**, 385–386.

Feely, O. & Chua, L. O. [1991] "The effect of integrator leak in $\Sigma\Delta$ modulation," *IEEE Trans. Circ. Syst.* **38**, 1293–1305.

Feely, O. [1992] "Nonlinear dynamics of sigma-delta modulation," *Proc. Midwest Symp. Circuits Syst.*, pp. 760–763.

Feigin, M. I. [1970] "Doubling of the oscillation period with C-bifurcations in piecewise-continuous systems," *Prikl. Math. Mekh.* **34**, 861–869 (in Russian).

Fermi, E. [1949] "On the origin of the cosmic radiation," *Phys. Rev.* **75**, 1169–1174.

Gardini, L., Tramontana, F., Avrutin, V. & Schanz, M. [2010] "Border collision bifurcations in 1D piecewise-linear maps and Leonov's approach," *Int. J. Bifurcation and Chaos* **20**, 3085–3104.

Gray, R. [1987] "Oversampled sigma-delta modulation," *IEEE Trans. Commun.* **35**, 481–489.

Jacomet, M., Goette, J., Zbinden, V. & Narvaez, C. [2004] "On the dynamic behavior of a novel digital-only sigma-delta A/D converter," *Proc. 17th Symp. Integrated Circuits and System Design*, Brazil, pp. 222–227.

Karner, G. [1994] "The simplified Fermi accelerator in classical and quantum mechanics," *J. Stat. Phys.* **77**, 867.

Lagarias, J. C. & Tresser, C. [1995] "A walk along the branches of the extended Farey tree," *IBM J. Res. Dev.* **39**, 283–294.

Leonel, E. D. & McClintock, P. V. E. [2006] "Dissipative area-preserving one-dimensional Fermi accelerator model," *Phys. Rev. E* **73**, 066223-1–066223-5.

Leonov, N. N. [1959] "Map of the line onto itself," *Radiofisika* **2**, 942–956 (in Russian).

Leonov, N. N. [1960a] "Map of the line onto itself," *Radiofisika* **3**, 496–510 (in Russian).

Leonov, N. N. [1960b] "Map of the line onto itself," *Radiofisika* **3**, 872–886 (in Russian).

Mira, C. [1987] *Chaotic Dynamics* (World Scientific, Singapore).

Mita, M., Arai, M., Tensaka, S., Kobayashi, D. & Fujita, H. [2003] "A micromachined impact microactuator driven by electrostatic force," *J. Microelectromech. Syst.* **12**, 37–41.

Nusse, H. E. & Yorke, J. A. [1992] "Border-collision bifurcations including "period two to period three" for piecewise smooth maps," *Physica D* **57**, 39–57.

Nusse, H. E., Ott, E. & Yorke, J. A. [1994] "Border-collision bifurcations: An explanation for observed bifurcation phenomena," *Phys. Rev. E* **49**, 1073–1076.

Peterka, F. [1974a] "Laws of impact motion of mechanical systems with one degree of freedom. Part I: Theoretical analysis of n-multiple $(1/n)$-impact motions," *Acta Technica CSAV* **4**, 462–473.

Peterka, F. [1974b] "Laws of impact motion of mechanical systems with one degree of freedom. Part II: Results of analogue computer modelling of the motion," *Acta Technica CSAV* **4**, 569–580.

Procaccia, I., Thomae, S. & Tresser, C. [1987] "First-return maps as a unified renormalization scheme for dynamical systems," *Phys. Rev. A* **35**, 1884–1900.

Reiss, J. D. & Sandler, M. B. [2001] "The benefits of multibit chaotic sigma delta modulation," *Chaos* **11**, 377–383.

Saif, F., Bialynicki-Birula, I., Fortunato, M. & Schleich, W. P. [1998] "Fermi accelerators in atom optics," *Phys. Rev. A* **58**, 4779–4783.

Stern, M. A. [1858] "Über eine zahlentheoretische Funktion," *J. Reine Angew. Math.* **55**, 183–220.

Zhao, X., Dankowicz, H., Reddy, C. K. & Nayfeh, A. H. [2004] "Modeling and simulation methodology for impact microactuators," *J. Micromech. Microeng.* **14**, 775–784.

Appendix A

Proof of Proposition 1

We have to demonstrate that for an arbitrary sequence σ, the sequences ρ and ρ' resulting from σ by replacements (64) and (66) are equivalent up to a cyclic shift: $\rho \equiv \rho'$. The proof for the replacements (65) and (67) is identical up to exchanging symbols $\mathcal{L}$ and $\mathcal{R}$. Note that for sake of clarity we write the index n instead of n_2 in replacements (64) and (66).

First we can exclude from the consideration the sequences $\mathcal{L}^k$ and $\mathcal{R}^k$ for any $k > 0$: in the first case, the replacements (64) and (66) lead to the same sequence $\rho = \rho' = (\mathcal{L}\mathcal{R}^n)^k$ and in the second case, we get

$$\begin{aligned}\rho &= (\mathcal{L}\mathcal{R}^{n+1})^k = \mathcal{L}\mathcal{R}^n(\mathcal{R}\mathcal{L}\mathcal{R}^n)^{k-1}\mathcal{R} \\ &\equiv (\mathcal{R}\mathcal{L}\mathcal{R}^n)^k = \rho' \end{aligned} \tag{A.1}$$

Hence, we have to consider only sequences σ containing both letters $\mathcal{L}$ and $\mathcal{R}$. It can be easily shown, that the sequence σ can be cyclically shifted so that it starts with the symbol $\mathcal{R}$ and ends with the symbol $\mathcal{L}$. Therefore it can always be written in the following form

$$\sigma \equiv \mathcal{R}^{m_1}\mathcal{L}^{p_1}\mathcal{R}^{m_2}\mathcal{L}^{p_2}\cdots\mathcal{R}^{m_k}\mathcal{L}^{p_k} \tag{A.2}$$

for some $k > 0$ and $m_i, p_i > 0$ with $i = 1, \ldots, k$. For $k = 1$ we have

$$\begin{aligned}\rho &= (\mathcal{L}\mathcal{R}^{n+1})^{m_1}(\mathcal{L}\mathcal{R}^n)^{p_1} \\ &= \mathcal{L}\mathcal{R}^n(\mathcal{R}\mathcal{L}\mathcal{R}^n)^{m_1-1}\mathcal{R}\mathcal{L}\mathcal{R}^n(\mathcal{L}\mathcal{R}^n)^{p_1-1} \\ &= \mathcal{L}\mathcal{R}^n(\mathcal{R}\mathcal{L}\mathcal{R}^n)^{m_1}(\mathcal{L}\mathcal{R}^n)^{p_1-1} \\ &\equiv (\mathcal{R}\mathcal{L}\mathcal{R}^n)^{m_1}(\mathcal{L}\mathcal{R}^n)^{p_1} = \rho' \end{aligned} \tag{A.3}$$

Similarly, for $k = 2$:

$$\begin{aligned}\rho &= (\mathcal{L}\mathcal{R}^{n+1})^{m_1}(\mathcal{L}\mathcal{R}^n)^{p_1}(\mathcal{L}\mathcal{R}^{n+1})^{m_2}(\mathcal{L}\mathcal{R}^n)^{p_2} \\ &= \mathcal{L}\mathcal{R}^n(\mathcal{R}\mathcal{L}\mathcal{R}^n)^{m_1-1}\mathcal{R}\mathcal{L}\mathcal{R}^n(\mathcal{L}\mathcal{R}^n)^{p_1-1} \\ &\quad \times \mathcal{L}\mathcal{R}^n(\mathcal{R}\mathcal{L}\mathcal{R}^n)^{m_2-1}\mathcal{R}\mathcal{L}\mathcal{R}^n(\mathcal{L}\mathcal{R}^n)^{p_2-1} \\ &= \mathcal{L}\mathcal{R}^n(\mathcal{R}\mathcal{L}\mathcal{R}^n)^{m_1}(\mathcal{L}\mathcal{R}^n)^{p_1}(\mathcal{R}\mathcal{L}\mathcal{R}^n)^{m_2}(\mathcal{L}\mathcal{R}^n)^{p_2-1} \\ &\equiv (\mathcal{R}\mathcal{L}\mathcal{R}^n)^{m_1}(\mathcal{L}\mathcal{R}^n)^{p_1}(\mathcal{R}\mathcal{L}\mathcal{R}^n)^{m_2}(\mathcal{L}\mathcal{R}^n)^{p_2} \\ &= \rho' \end{aligned} \tag{A.4}$$

and for any $k > 2$ the proof is completely analogous. ■